Ecological Modelling 512 (2026) 111390

Contents lists available at ScienceDirect

Ecological Modelling

journal homepage: www.elsevier.com/locate/ecolmodel

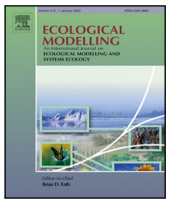

Modeling canopy-forming *vs*. turfing algae competition via a space-implicit model with border dynamics

D. Collini [a], L. Barletti [a], F. Bulleri [b], S. Dalmazzone [c], V. Frontuto [c], L. Tamburello [d,e], F. Sarnari [f], M. Materassi [g,*]

[a] University of Florence, Department of Mathematics and Computer Science, Florence, 50134, Italy
[b] University of Pisa, Department of Biology, Pisa, 56126, Italy
[c] University of Turin, Department of Economics and Statistics (ESt), Turin, 10153, Italy
[d] Stazione Zoologica Anton Dohrn, Department of Integrative Marine Ecology, Sicily, Lungomare Cristoforo Colombo, Palermo, 90142, Italy
[e] NBFC, National Biodiversity Future Center, Palermo, 90133, Italy
[f] Institute of molecular bioimaging and physiology of the National Research Council (CNR-IBSBC), Cefalu, Palermo, 90015, Italy
[g] Institute for Complex Systems of the National Research Council (CNR-ISC), Florence, 50019, Italy

ARTICLE INFO

Keywords:
Trophic webs
Pack behavior
Cystoseira
Kelp
Inter-algal competition
Environmental bio-indicators
Edge effects
Marine biodiversity

ABSTRACT

This paper presents a model of competition between arborescent canopy-forming algae (such as Fucales of genus *Cystoseira s.l.* or Laminariales of genus *Laminaria*), and the smaller size algae forming turf on rocky bottoms. The two algal assemblages are both grazed by sea urchins. The model is a 3-species space-implicit food web, and its distinctive feature is the inclusion of community border effects in interactions: the individuals laying along the canopy border take part in recruitment and competition with algal turfs, and undergo grazing by sea urchins, much more efficiently than algae in the canopy bulk. Also the endogenous recruitment of turf takes place mostly along the border of the turf area. The prevalence of these edge effects is taken into account by supposing that the processes affected by them involve only border individuals and is described in the same way herd behavior is treated in the mathematical ecology of animals. It is shown that the border effect inclusion does make a difference in terms of phase space structures, hence in the ecological scenarios it predicts. Various features of the phase space of the proposed system are investigated, focusing on the capacity of this model to mimic the transitions among ecologically different states of the rocky bottom (coexistence of canopy and turf, survival of the turf only, bare rocky bottom).

The algae and invertebrates involved in the model play an important role in the health of coastal ecosystems and particularly in the conservation of biodiversity-rich habitats of temperate nearshore rocky reefs. Hence, the model presented may contribute to a deeper understanding of ecological processes underlying canopy degradation and recovery, and provide a framework for their management in future applications.

1. Introduction

Macroalgal forests of canopy-forming species belonging to the orders Laminariales (i.e., kelps) or Fucales (namely species belonging to the complex *Cystoseira sensu lato*, including the genera *Cystoseira*, *Ericaria* and *Gongolaria*, see e.g. Molinari-Novoa and Guiry, 2020) are among the most diverse and productive coastal systems. Nonetheless, they are declining globally as a consequence of human alteration of both biotic and abiotic conditions, including climate changes, eutrophication, overgrazing by urchins, enhanced sediment loads, chemical pollution and urbanization (Krumhansl et al., 2016). Macroalgal forest decline can take the form of a system transition leading to two possible alternative states dominated, respectively, by either encrusting coralline, or turf-forming macroalgae (Benedetti-Cecchi et al., 2001; Gorman and Connell, 2009; Strain et al., 2014; Ling et al., 2015).

Encrusting coralline dominance is generally the result of the overgrazing of erect algal forms by marine herbivores, often sea urchins, triggered by the over-exploitation of their predators (Bulleri and Benedetti-Cecchi, 2006).

In contrast, alteration of environmental conditions, such as nutrient loading and enhanced sedimentation, can promote the shift from macroalgal forests to turfs composed of opportunistic forms generally characterized by high efficiency of resources, year-round sexual reproduction, vegetative propagation and stress tolerance (Gorman and Connell, 2009). Once established, algal turfs can prevent the recovery

* Corresponding author.
E-mail address: massimo.materassi@cnr.it (M. Materassi).

https://doi.org/10.1016/j.ecolmodel.2025.111390
Received 5 December 2024; Received in revised form 30 September 2025; Accepted 21 October 2025
Available online 9 November 2025

of canopy-forming species through the space pre-emption and the trapping of sediments (Airoldi, 1998; Alestra and Schiel, 2015).

Transitions in the state of ecosystems driven by human perturbations have been documented in terrestrial and aquatic habitats, including forests, savannas, deserts, lakes, coral reefs and macroalgal forests (Scheffer et al., 2001; Bestelmeyer et al., 2011 and references therein). Understanding the mechanisms underpinning shifts to degraded states, and the nature of reinforcing feedback dynamics that sustain their persistence, is key to safeguarding the biodiversity and functioning of ecosystems and the services they provide (Balvanera et al., 2006; Worm et al., 2006; Selkoe et al., 2015). Ecosystem mathematical modeling through the theory of dynamical systems may help represent and understand ecosystem shifts (Ratajczak et al., 2018).

To anticipate how canopy ecosystems respond to human-driven disturbances, interactions between invertebrate grazers – such as sea urchins – and canopy-forming species have been widely investigated across temperate reefs worldwide. Notable case studies include Canada (Lauzon-Guay et al., 2009; Baskett and Salomon, 2010), Chile (Ortiz and Uribe, 2021), California (Karatayev and Baskett, 2020; Dunn et al., 2021), Tasmania (Marzloff et al., 2013; Wilman, 2021), and the Mediterranean Sea (Rustici et al., 2017; Melis et al., 2019).

Models have described shifts of the system driven by depletion of sea urchins' predators due to overfishing (Dunn et al., 2021; Marzloff et al., 2013; Rustici et al., 2017) or to climate-related overgrazing (Lauzon-Guay et al., 2009; Wilman, 2021), providing valuable insights for the management of forested systems. There exists a wide literature with reference to the Mediterranean context, where Fucales, and *Cystoseira s.l.* in particular, are more widespread than Laminariales: this documents the canopy-forming algae relevance in sustaining biodiversity and ecosystem services (Cheminée et al., 2013; Sala et al., 2012; Thiriet et al., 2016; Cheminée et al., 2013), and their vulnerability to climate changes (e.g. Lardi et al., 2022) and anthropogenic disturbances, such as eutrophication, overgrazing by urchins, enhanced sediment loads, chemical pollution and urbanization (Thibaut et al., 2005, 2014; Ballesteros et al., 2007). Several models have fine-tuned the ecological framework incorporating facilitative interactions (Baskett and Salomon, 2010), dispersal processes or recruitment variability (Karatayev and Baskett, 2020; Dunn et al., 2021), predators and prey behavior (Dunn et al., 2021; Melis et al., 2019), or additional human pressures, e.g., eutrophication (Boada et al., 2017) and kelp harvesting (Dunn et al., 2021; Ortiz and Uribe, 2021).

To the best of our knowledge, however, no model has taken into account that rocky reef assemblages are often composed of a mosaic of patches of alternative habitats (Bulleri and Benedetti-Cecchi, 2006), and that some of the key processes underpinning state transitions mainly involve the individuals located along their borders.

In order to deepen our understanding of edge-effect driven processes, we want to investigate how incorporating explicitly the edge effects in the ecological model of Fucales canopies on rocky reefs influences the resulting dynamics. Using as a model system Mediterranean coastal environments, mainly populated by algal forests of *Cystoseira s.l.*, we developed a space-implicit model of the dynamics of macroalgal assemblages by constructing a web of functional group interactions occurring at the boundary between forest and turf patches.

In our model, we have assumed that: (i) *Cystoseira s.l.* recruitment, (ii) grazing of *Cystoseira s.l.* by sea urchins, (iii) competition with algal turfs and (iv) vegetative expansion of algal turfs only occur at the boundaries between forest and turf patches, or forests and sea urchin packs. We want to show that models not doing so, i.e. assuming that all the bulk individuals take part in canopy recruitment, grazing, competition and turf expansion, will lead to representing the dynamical interactions between the three communities in a quantitatively different way. They, for example, may overestimate the equilibrium value of canopy populations, or miss the appearance of limit cycles, and thus may convey misleading predictions and policy implications different from those of the edge interaction model. Clearly, only a direct comparison of the model predictions with real data, outside the scope of this paper, could define which is the correct model. However, here we establish that the inclusion of edge interactions in a mathematically consistent way makes a sensible, possibly measurable, difference.

2. Methods

The model presented here is a space-implicit model of the dynamics of the population abundances, mathematically represented by C (*Cystoseira s.l.*), T (turf) and U (sea urchins) in arbitrary units. Arbitrary units may not sound predictive, but they render the model scalable within the limits of validity of the assumptions made.

The three "populations" C, T and U are all species communities, not including single species taxonomically intended: *Cystoseira s.l.* includes different genera (i.e., *Cystoseira*, *Ericaria* and *Gongolaria*, see Molinari-Novoa and Guiry, 2020); turf is itself a collection of different co-living algae; sea urchins are a group of different species represented with a unique behavior, even if some differences exist among them. For instance, in the Mediterranean shallow reefs there exist the two species *Paracentrotus lividus* and *Arbacia lixula*, *P. lividus* being the more abundant of the two. In reality, the two sea urchin species have slightly different behavior: *P. lividus* usually grazes on the turf and at the border of the *Cystoseira s.l.* canopy, while *A. lixula* lives more on the barren (Bulleri, 2013; Bulleri et al., 2020; Bevilacqua et al., 2021). *A. lixula* may graze juveniles of *Cystoseira s.l.*, but cannot consume adult algae. Yet, in our model the grazing pressure on the canopy is represented as the effect of a unique guild of sea urchins. Both these species may eventually be found in the inner part of *Cystoseira s.l.* canopies, but in our model sea urchins are simply supposed to graze only either the epiphytes or the understorey, without consuming arborescent algae inside the canopy.

The choice to represent the extended ecosystem (living on a portion of the sea floor) through a space-implicit model is due to the fact that it is simpler to find a way to encode border interactions in such a lumped parameter model with ordinary differential equations (ODEs), than in a space-explicit model with partial derivative differential equations (PDEs). In fact, the border along which these interactions should be located is not a well-defined geometrical place assigned rigidly, or easy to characterize in terms of local properties, but a curve on the sea floor plane depending on the population densities and locations themselves: expressing this in mathematics needs non-local terms involving density gradients, hence producing a model too far from the reasonable simplicity we would like to have (even if the theory of free boundary dynamics might help in making it via PDEs, see e.g. Fasano and Primicerio, 1979).

A space-implicit dynamical system allows for the inclusion of border interactions through the simple dimensional reasoning reported in Appendices A.2 and A.4. Basically, if X is the value of the total number of individuals, or total biomass, of a given species living on a 2-dimensional region of the sea floor, the same quantity pertaining only to those living on the border, indicated as X_∂, is assumed to be proportional to the square root of X Ajraldi et al. (2011):

$$X_\partial = k\sqrt{X}. \tag{1}$$

Let the population state variable X (i.e. C, T or U here) be the total biomass of this population: then, one has $X = m_x n_x$, being n_x the number of individuals and m_x their (average) mass. The relationship (1) should be strictly intended between n_x and the number of border individuals $(n_x)_\partial$, as:

$$(n_x)_\partial = k_n\sqrt{n_x}.$$

On the other hand, the total border mass is simply

$$X_\partial = m_x\,(n_x)_\partial = k_n m_x\sqrt{n_x},$$

so that one recognizes

$$\text{Eq. (1)} \iff k = k_n\sqrt{m_x}. \tag{2}$$

The condition (2) ensures that X and X_∂ have the same dimension, because they are both biomasses. The question may arise about the value, dimensions and units for the coefficients appearing in the response functions, when either border or bulk populations are involved. This issue is discussed thoroughly in Appendix B. All in all, one may safely state that the relationship (1) holds both for the number of individuals and the total biomass, provided the conversion (2) is taken into account.

The X-independent coefficient k in (1) is a form factor related to the geometrical shape of the 2D-region inhabited by X (for instance, it is easy to show that one has $k = 2\lambda\sqrt{\frac{m_X \pi}{\sigma}}$ if X occupies a disk, being λ the number line density of individuals along the circumference, and σ the number surface density within the round area).

In our model the factor k is considered just as a constant that does not depend on the population dynamics, and remains equal all over its evolution. This is equivalent to stating that the 2D-regions inhabited by the populations C, T and U have all the same, constant shape. This is sensible, as far as those factors can be included in the parameters appearing in front of X_∂. As in the joke of the theoretical physicist exactly predicting the winner of any horse race, provided horses are all spheres, here we are implicitly assuming that all the *Cystoseira s.l.* canopies have the same 2D-shape, and so do the turf regions and sea urchin packs. Even though this may seem oversimplified, the purpose here is just to discuss how a basic implementation of edge interactions through topological considerations can be done, leaving refinements for more realistic geometries to forthcoming studies. The key condition to include the form factor k in the model constant parameters is that the shape of canopies and packs must remain constant along the system evolution, so that no further geometrical subtleties, moreover depending on dynamics, arise. Throughout our discussion, a round, or square, canopy is assumed to stay round, or square, all along the evolution of the ecosystem, and so do the turf patches and sea urchin packs. What is neglected in the model is any dependence of the shape of the algal areas or sea urchin packs on their own size, as $k(X)$ in Eq. (1). Such a dependence on $k(X)$ could be expected in principle, but is not documented in any marine biology literature to our best knowledge, and hence is not included in the present model. This does not exclude further investigations on this point to be reported in future works.

2.1. Model zoology

Let us now present the model equations involving the three variables C, T and U. These equations have been constructed through the reasoning and assumptions presented in the Appendix A. They include reciprocal shadowing between the two algae through the attenuation factors $\xi(T)$ and $\eta(C)$; endogenous recruitment of the two algae, due to the border individuals only; exogenous recruitment of turf; border competition between the two algae; border grazing of sea urchins on *Cystoseira s.l.* and bulk grazing of sea urchins on turf; sea urchin natural mortality. All in all, they read:

$$\begin{cases} \dfrac{dC}{dt} = \xi(T)\, R_C \sqrt{C}\left(1 - \sqrt{\dfrac{C}{K_C}}\right) - f_{CU}\left(\sqrt{C}\right)\sqrt{U} - \beta\sqrt{CT}, \\ \dfrac{dT}{dt} = \eta(C)\,\Phi\left(1 - \dfrac{T}{K_T}\right) + R_T\sqrt{T}\left(1 - \sqrt{\dfrac{T}{K_T}}\right) - f_{TU}(T)\,U, \\ \dfrac{dU}{dt} = c_{CU} f_{CU}\left(\sqrt{C}\right)\sqrt{U} + c_{TU} f_{TU}(T)\,U - \Delta_U U \end{cases} \tag{3}$$

(note the presence of a disadvantageous addendum $-\beta\sqrt{CT}$ in the ODE of C, which is not matched by any term in the ODE of T: this is because the propagules of *Cystoseira s.l.* are supposed not to survive falling in the turf region, while the opposite does not happen, making the C *vs.* T border competition asymmetric). The meaning of all the parameters of the model are explained in Table 1.

Table 1
Elencation of the model parameters with their physical meaning explained.

Parameter	Meaning
T_0, T_0^*	Shadowing scale of turf on *Cystoseira s.l.*, for the exponential and algebraic form
R_C	Stand-alone growth rate of *Cystoseira s.l.*
K_C	Stand-alone carrying capacity of *Cystoseira s.l.*
β	Coefficient of the border competition of turf on *Cystoseira s.l.*
C_0, C_0^*	Shadowing scale of *Cystoseira s.l.* on turf, for the exponential and algebraic form
Φ	Stand-alone growth rate for exogenous recruitment of turf
K_T	Stand-alone carrying capacity of turf
R_T	Stand-alone growth rate of turf
c_{CU}	Metabolic factor of conversion of *Cystoseira s.l.* biomass into the sea urchin one
c_{TU}	Metabolic factor of conversion of turf biomass into the sea urchin one
Δ_U	Stand-alone mortality inverse time for sea urchins
a_{CU}	Constant *pro capite* grazing rate of insatiable sea urchins on *Cystoseira s.l.*
a_{TU}	Constant *pro capite* grazing rate of insatiable sea urchins on turf
A_{CU}	Asymptotic *pro capite* grazing rate of satiable sea urchins on *Cystoseira s.l.*
B_{CU}	Value of *Cystoseira s.l.* abundance so that its pro capite consumption is $\frac{A_{CU}}{2}$
A_{TU}	Asymptotic *pro capite* grazing rate of satiable sea urchins on turf
B_{TU}	Value of turf abundance so that its pro capite consumption is $\frac{A_{TU}}{2}$

The response functions f_{CU} and f_{TU} are respectively the *pro capite* rate of grazing of sea urchins on *Cystoseira s.l.* and turf: if these functions grow indefinitely with the abundance of the grazed alga, one speaks about insatiable sea urchins:

$$f_{CU}\left(\sqrt{C}\right) = a_{CU}\sqrt{C},\ f_{TU}(T) = a_{TU}T. \tag{4}$$

namely Holling Type I expressions. If the response functions tend to saturate for growing $\sqrt{C}$ and T respectively, the grazers are referred to as satiable, and the f_{CU} and f_{TU} are Holling Type II expressions:

$$f_{CU}\left(\sqrt{C}\right) = \frac{A_{CU}\sqrt{C}}{B_{CU} + \sqrt{C}},\ f_{TU}(T) = \frac{A_{TU}T}{B_{TU} + T}. \tag{5}$$

The two attenuation factors $\xi(T)$ and $\eta(C)$ due to reciprocal shadowing may be taken either as algebraic expressions:

$$\xi(T) = 1 - \frac{T}{T_0^*},\ \eta(C) = 1 - \frac{C}{C_0^*}, \tag{6}$$

or as exponential ones:

$$\xi(T) = e^{-\frac{T}{T_0}},\ \eta(C) = e^{-\frac{C}{C_0}}, \tag{7}$$

see Appendix A for further details. Our interest is to discuss the (C, T, U) system, with the exponential form (7) for the attenuation factors is used, and the satiable grazer response functions (5), so that the dynamics reads:

$$\begin{cases} \dfrac{dC}{dt} = e^{-\frac{T}{T_0}} R_C\sqrt{C}\left(1 - \sqrt{\dfrac{C}{K_C}}\right) - \dfrac{A_{CU}\sqrt{CU}}{B_{CU} + \sqrt{C}} - \beta\sqrt{CT}, \\ \dfrac{dT}{dt} = e^{-\frac{C}{C_0}}\Phi\left(1 - \dfrac{T}{K_T}\right) + R_T\sqrt{T}\left(1 - \sqrt{\dfrac{T}{K_T}}\right) - \dfrac{A_{TU}TU}{B_{TU} + T}, \\ \dfrac{dU}{dt} = c_{CU}\dfrac{A_{CU}\sqrt{CU}}{B_{CU} + \sqrt{C}} + c_{TU}\dfrac{A_{TU}TU}{B_{TU} + T} - \Delta_U U. \end{cases} \tag{8}$$

Last but not least, one may be interested either to the description of the simple *Cystoseira s.l.* versus turf competition, with the sea urchin

abundance U considered as a parameter (the 'constant-U' model), or to the complete dynamics of the (C,T,U) system, in which U is a proper dynamical variable (the 'complete' model). A U-constant model is described in Appendix C.

The choice of the attenuation factor ξ and η form for the different versions of the model is guided by the principle of simplicity: the exponential form (7) is more physical, as it recalls the attenuation of light through a medium, being shadowing competition just the light attenuation through the substance of epiphytes or the branches of *Cystoseira s.l.* individuals. However, the analytical manipulation of these equations is only possible when adopting the algebraic form (6). Hence, our choice is to use the algebraic form together with the insatiable sea urchin approximation, a combination that makes the analytical manipulation of the system readily feasible, as illustrated in the 2D sub-model presented in Appendix C.

The exponential attenuation (7) can instead be employed in the satiable urchin form of the ODEs, where more complicated equations would anyhow require to be dealt with numerically. A full treatment of the different cases, studied either numerically, or analytically when possible, was developed in the mathematical study (Collini, 2019).

As the whole paper is devoted to assessing the effects of recognizing the border interactions by using the border populations calculated as in (1), it will be useful to make a comparison with the version of the same trophic web in which the bulk populations C, T and U simply replace their boundary portions $\sqrt{C}$, $\sqrt{T}$ and $\sqrt{U}$ in (8), giving:

$$\begin{cases} \dfrac{dC}{dt} = R_C e^{-\frac{T}{T_0}} C\left(1-\dfrac{C}{K_C}\right) - \beta CT - \dfrac{A_{CU}CU}{B_{CU}+C}, \\ \dfrac{dT}{dt} = \Phi e^{-\frac{C}{C_0}}\left(1-\dfrac{T}{K_T}\right) + R_T T\left(1-\dfrac{T}{K_T}\right) - \dfrac{A_{TU}TU}{B_{TU}+T}, \\ \dfrac{dU}{dt} = C_{CU}\dfrac{A_{CU}CU}{B_{CU}+C} + C_{TU}\dfrac{A_{TU}TU}{B_{TU}+T} - \Delta_U U. \end{cases} \tag{9}$$

The analysis of the system's behavior (9), in comparison with that of (8), is presented in Results. The results are recognizably different, supporting the conclusion that boundary interactions play a significant role. As anticipated, only comparison of the predictions of models (8) and (9) with empirical data could determine which is more appropriate; the aim here is solely to establish that quantitative differences do exist.

The system (8) may also be related to space-implicit one-predator–two-prey models that incorporate different types of interactions between the prey populations. In the literature reviewed here, the specific mechanisms underlying (8) – namely, competition that nonlinearly attenuates growth rates and border competition – are not considered. Furthermore, limit cycles are rarely reported in such models (Colucci et al., 2021), whereas in our case they do emerge for appropriate parameter choices of system (8) (see Results for details). From an ecological perspective, limit cycles are particularly relevant, as they correspond to periodic oscillations in population abundances and community states, shaping the long-term dynamics and stability of ecosystems (May, 1974).

The model dynamics described above are explored through numerical simulations. The code was written in Matlab© programming language, and is available, for reproducibility, at https://github.com/Bar68/Cystoseira.git. The solver used is the built-in function *ode45* which performs discretization through an adaptive step-size Runge–Kutta method. The intervals of variation of C, T, and U explored in our simulations are intended as reference values, without a strict experimental correspondence to real ecosystems. Establishing such correspondence will be the subject of future work, at aimed at facilitating comparison with field data.

As anticipated in the Introduction, our purpose is to present a novel model, demonstrate the significance of border interactions in shaping its behavior, and highlight how different ecological scenarios can arise through appropriate parameter selection. The two scenarios explored here are referred to as $\Sigma_{1,2}$ and their dynamics and coefficient values are summarized in Table 2.

Table 2
The parameter values of the model are summarized for all its variants. Σ_A denotes the U-constant model with algebraic attenuation functions and insatiable sea urchins; Σ_B denotes the U-constant model with algebraic attenuation functions and satiable sea urchins; Σ_1 and Σ_2 correspond to the full model with exponential attenuation functions and satiable sea urchins. Finally, Σ_3 represents the model with the same parameters as Σ_1, but incorporating only bulk interactions. The reference equations for each scenario are provided in the second row of the table under "ODEs (...)". Empty cells indicate parameters that are not applicable to the corresponding scenario (e.g., c_{CU} for Σ_A, i.e., the system governed by ODEs (C.1)).

Parameter	Value in Σ_A ODEs (C.1)	Value in Σ_B ODEs (C.2)	Value in Σ_1 ODEs (8)	Value in Σ_2 ODEs (8)	Value in Σ_3 ODEs (9)
T_0, T_0^*	$T_0^* = 2$	$T_0^* = 5$	$T_0 = 2$	$T_0 = 10$	$T_0 = 2$
R_C	5	1.5	1.5	3	1.5
K_C	1	1	1	1	1
β	1	0.1	0.1	0.1	0.1
C_0, C_0^*	$C_0^* = 1$		$C_0 = 3$	$C_0 = 3$	$C_0 = 3$
Φ	1	0.1	0.2	4.5	0.2
K_T	1	1	1	1	1
R_T	1	1	1	4.5	1
c_{CU}			0.9	0.9	0.9
c_{TU}			0.9	0.9	0.9
Δ_U			3.52	1	3.52
a_{CU}	1				
a_{TU}	1				
A_{CU}		1	1	1	1
B_{CU}		0.1	0.1	0.8	0.1
A_{TU}		1	1	3	1
B_{TU}			0.6	0.6	0.6
U	1	0.1			

The scenarios Σ_A and Σ_B pertain to the dynamics of the 2D sub-model described in Appendix C, with a constant population U of insatiable and satiable sea urchins respectively.

The scenarios Σ_1 and Σ_2 indicated in Table 2 are given by two parameter sets in the same dynamical system (8), where the three populations C, T and U are all dynamical variables, sea urchins are supposed satiable, and the reciprocal shadowing of *Cystoseira s.l.* and turf is represented through exponential attenuation factors. Section 3.1 reports results about the simulated scenarios Σ_1 and Σ_2.

The final condition simulated corresponds to the scenario labeled Σ_3 in Table 2. In this case, the dynamics follow system (9), while the coefficients are the same as in scenario Σ_1. In Σ_3, border interactions are replaced by bulk interactions, sea urchins remain satiable, and shadowing attenuation is exponential. The results of scenario Σ_3 are presented in Section 3.2, where comparison with Σ_1 clearly illustrates the contribution of border interactions relative to bulk interactions, at least from a mathematical perspective.

3. Results

In this Section we present the results obtained through numerical simulations of the modeled dynamics. It is important to emphasize that the phase space structures identified in our analysis are all stable under the model's dynamics: these structures were indeed revealed by systematically running a large number of simulations across the widest possible assortment of initial conditions. This brute-force approach ensures that even partly unstable loci, such as saddle points, are naturally excluded.

3.1. Results on the model with edge interactions

Let us now present the numerical analysis of the complete (C,T,U) model. For reference, the portion of the (C,T,U) phase space explored

here is $C \in [0,1]$, $T \in [0,1]$, and $U \in [0,3]$. While this choice necessarily excludes the exploration of wider regions, it nonetheless provides a meaningful investigation of the ecological conditions potentially represented by model (8). We test various parameter combinations, allowing the model to exhibit different attractors and, consequently, represent distinct ecological scenarios

A first parameter choice for the system is the one reported in column Σ_1 of Table 2. This gives rise, within the subset of the phase space $[0,1]\times[0,1]\times[0,3]$, to two stable pointlike asymptotic equilibria with no sea urchin $E_1 = (0,1,0)$ and $E_2 = (0.79, 0.99, 0)$, and a limit cycle along which no population goes extinct. The plot of these three attractors is reported in Fig. 1, and a sample trajectory attracted by the limit cycle is shown in Fig. 2.

The three attractors of the phase space subdivide the latter into three stability domains. These basins have been identified via multiple numerical simulations and represented in Fig. 3, where initial conditions lying in the red domain of the diagram lead to the equilibrium E_1, those in the blue domain are attracted to the limit cycle, and those in the green plane end up in the E_2 equilibrium. Fig. 4 shows the same basins of attraction through sections at constant $U > 0$ of the same portion of the phase space as in Fig. 3. Each section reports for a different value of U the regions of the CT-plane containing the initial conditions from which the system converges to E_1 (upper-left regions) or to the limit cycle (lower-right regions). Therefore, a thick region is attracted by the equilibrium where only the turf survives, competing with that attracted by the limit cycle. For $U = 0$ (not shown in the figure), all initial conditions with $C > 0$ are attracted by E_2 and only the initial $C = 0$ converges to the same E_1 in Fig. C.6 (where this point is indicated as X_1).

The structure and size of the basins of attraction depend on the choice of parameters. The presence of the limit cycle itself is sensitive to the values of the model's coefficients. Let us examine how this phase space structure varies with three parameters that are of particular ecological interest: the growth rate R_C of isolated *Cystoseira s.l.*, the extinction rate Δ_U of isolated sea urchins, and the growth rate due to propagules carried by currents Φ of isolated turf (with the term "isolated", or "stand alone", here we mean "in the absence of the other two populations": for instance, if one sets $C = 0$ and $T = 0$ in the model equations, sea urchins get extinct by starvation at an exponential rate with characteristic inverse time equal to Δ_U). The parameters we are discussing are interesting from the perspective of an environmental management use of some future developments of the model: the *Cystoseira s.l.* growth rate R_C depends on the health state of *Cystoseira s.l.* forests (influenced by, e.g., the incidence of local stressors such as eutrophication, water turbidity, or pollutants); the flux of turf propagules Φ depends both on the presence of distant turf colonies releasing propagules, and on sea currents (yet, there cannot be a $\Phi = 0$ condition due to currents, as turf algae are always present as epiphytes or undergrowth in the *Cystoseira s.l.* canopy, and a $\Phi \neq 0$ may be due to this fact). Finally, the inverse of the sea urchin starvation time, Δ_U, may depend on environmental conditions affecting urchin health as well as on fishing pressure – either directly on sea urchins (where increased urchin fishing raises Δ_U) or on their predators (where greater fishing of predator species reduces Δ_U). Consequently, the three parameters R_C, Φ, and Δ_U can capture the influence of anthropogenic effects.

A bifurcation study of the model (8) against the variation of these parameters could allow to check indirectly which intervals of anthropic pressure or natural processes may cause the limit cycle to emerge. For conditions including the scenario in Fig. 1, one keeps two of the three parameters (R_C, Φ, Δ_U) fixed as in the scenario Σ_1, and leaves the other one span over some interval, within which a sub-interval is singled out where the limit cycle exists. The results are represented in Fig. 5, where one varies a single parameter at a time.

The quasi-planar nature in the (C,T,U) phase space of the limit cycle discovered for this system around the conditions of column Σ_1 in Table 2 is accurately discussed in the study (Collini, 2019).

The last scenario we want to report for the model in (8) describes the situation of full coexistence of three constant populations, with a unique asymptotically stable pointlike equilibrium within the phase space region spanned by our simulations. As we frequently observe "static" co-existence in nature, the parameters are chosen with an eye on realistic conditions. The shadowing of *Cystoseira s.l.* on the undergrowth of turf is taken to be more effective than the shadowing of turf algae as epiphytes of *Cystoseira s.l.*. Moreover in real situations both the border growth rate of turf and the exogenous contribution are stronger than that of *Cystoseira s.l.*. Respecting prescriptions motivated by these realistic ecological considerations – namely, $\eta(C) < \xi(T)$, $R_T > R_C$ and $\Phi > R_C$ – the parameter set is selected (among many other possibilities) as shown in column Σ_2 of Table 2.

By choosing the parameters in this way, only a single fixed point appears, with coordinates $E_0 = (0.13, 0.28, 4.38)$, where all three populations coexist. Within the numerically explored ranges of C, T, and U, this equilibrium – observed in simulations of the current scenario – appears to be global. Importantly, E_0 is the only asymptotically stable equilibrium to which (C,T,U) converges when starting with $C > 0$ and $U > 0$. In contrast, starting with $C = 0$ or $U = 0$ leads to C-free or U-free equilibria, respectively.

3.2. Results on the model with bulk interactions

Although a full analysis of the pure bulk version (9) of our system is beyond the scope of this paper, we aim to provide a glimpse of how its phase space differs from that of (8). To this end, we simulate system (9) using the same parameters as in scenario Σ_1, i.e., under the conditions corresponding to Σ_3 in Table 2. For this bulk version of the system, the asymptotically stable equilibria within the explored region $[0,1]\times[0,1]\times[0,3]$ of the (C,T,U) space are two fixed points with coordinates $F_1 = (0,1,0)$ and $F_2 = (0.89, 1, 0)$. No limit cycle is observed for the range of initial conditions considered. The absence of the limit cycle represents a striking difference between the border interaction system (8) and its bulk interaction counterpart (9), underscoring the critical role of border effects.

It is also important to comment on the coordinates of $F_{1,2}$, pointlike equilibria of the system (9), with respect to the coordinates of $E_{1,2}$ obtained for the system (8). The points E_1 and F_1 are the same "trivial equilibrium" $(C_{eq}, T_{eq}, U_{eq}) = (0, K_T, 0)$ for (8) and (9), that is $E_1 = F_1 = (0,1,0)$ for the choice Σ_1 of the model parameters. The point E_2 equilibrating (8) and F_2 equilibrating (9) are different, and read:

$$E_2 = (0.79, 0.99, 0)\,, \quad F_2 = (0.89, 1, 0)\,.$$

It is worth noting that $C(E_2) < C(F_2)$. Apparently, in the U-free state where *Cystoseira s.l.* coexists with the turf, the bulk interaction model (9) supports a larger canopy with the same saturating turf $T = K_T = 1$. A sensible explanation for this is that in system (8) only border individuals of the canopy contribute to Fucales recruitment, while in system (9) the whole *Cystoseira s.l.* populations gives rise to new biomass. The fact that sea urchin grazing on the canopy is more severe in system (9) than in system (8) does not influence the first coordinate of E_2 and F_2, as these are U-free equilibria, that is, no-grazing states.

4. Discussion

The model presented here offers a space-implicit representation of the interactions between macroalgal groups – *Cystoseira s.l.* and turf algae – and their primary herbivores, the sea urchins *Paracentrotus lividus* and *Arbacia lixula*, which are treated collectively as a single sea urchin population.

In nature, there is clear evidence that key ecological processes – such as the recruitment of canopy-forming algae, grazing by sea urchins, and competition between canopy and turf species – primarily

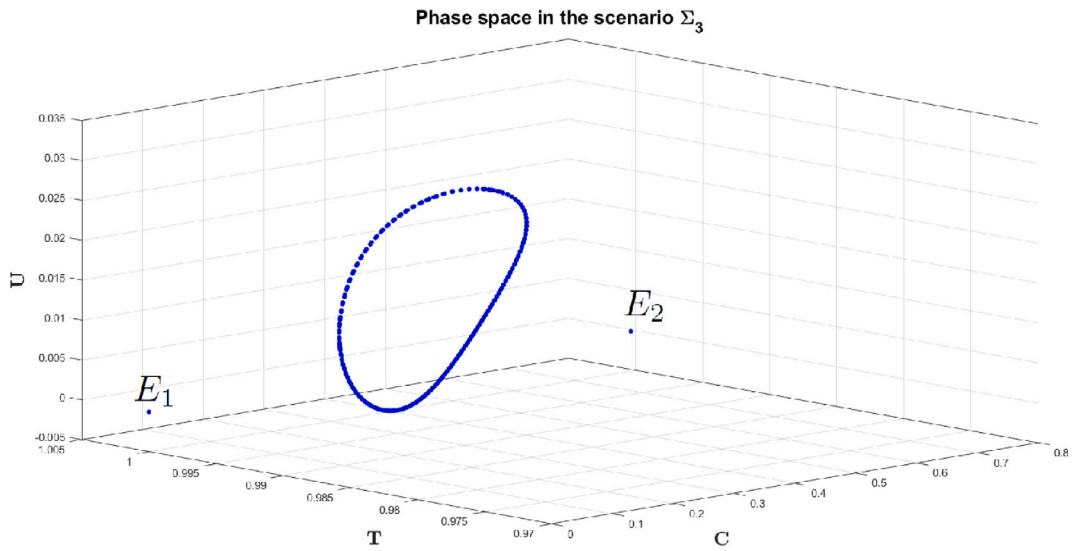

Fig. 1. Phase portrait of the system, with the parameters set as in the scenario Σ_1 of (Table 2): the C, T and U axes represent the *Cystoseira s.l.*, turf and sea urchin population respectively. Parameters are chosen in order to have two asymptotic equilibria E_1 and E_2, and a limit cycle (namely, the system (8). In E_1 and E_2 sea urchins have got extinct, and in E_1 also the *Cystoseira s.l.* has disappeared. The loop in the bulk of the (C, T, U) space is the limit cycle, along which the three populations periodically cycle with time.

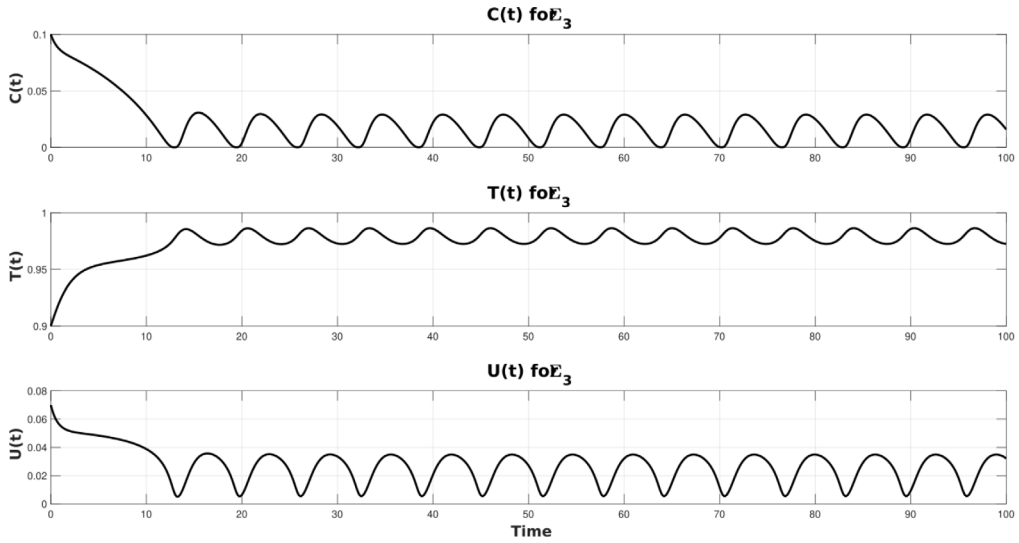

Fig. 2. A sample trajectory converging to the limit cycle of Fig. 1: from the top to the bottom, the evolution with time (in arbitrary units) of *Cystoseira s.l.*, turf and sea urchin populations (also in arbitrary units). The minimum values of $C(t)$, that never truly vanishes, is $C_{\min} = 6.68 \times 10^{-5} \neq 0$.

occur at the boundaries of the seabed areas occupied by each population. Therefore, the main goal of our work is to assess the impact of explicitly incorporating border interactions, as opposed to assuming only bulk (mean-field) interactions among populations. Our results show that including border dynamics fundamentally alters the structure of the phase space of the dynamical system, leading to behaviors that are markedly different from those predicted by a bulk interaction model.

In the context of ecosystem transitions, such edge effects have been claimed to play a key role in the recovery of perturbed populations (Petraitis and Latham, 1999; Ries et al., 2004; Knowlton, 2004; Fagan et al., 1999). Edge effects affecting the distribution of sea urchins and their grazing activity have been experimentally observed at the boundary between seagrass meadows and rocks (Bulleri, 2013; Pinna et al., 2013; Pages et al., 2014), and at the boundary between macroalgal forests and barrens (Konar and Estes, 2003; Ling et al., 2019). Likewise, due to the limited dispersal of canopy alga embryos and their small probability of survival when they fall within the shadowed internal canopy (Verdura et al., 2018; Falace et al., 2018), individuals at forest edges are likely to make a larger contribution to the expansion of forest patches through the recruitment of new individuals. Edge effects are also critical in the recovery of forests following disturbances (Tamburello et al., 2019a) or sea urchin removal (Piazzi and Ceccherelli, 2019; Bulleri and Benedetti-Cecchi, 2006).

To describe algal competition, recruitment, and sea urchin grazing, we drew on geometric considerations commonly used in modeling herd behavior in animal ecology (Ajraldi et al., 2011). This approach leads to the inclusion of terms in the model equations involving the canopy border population C_∂, the turf border population T_∂, and the sea urchin border population U_∂, rather than the total populations C, T, and U. Accordingly, the border populations are expressed in terms of the total populations as $C_\partial = k\sqrt{C}$, $T_\partial = k\sqrt{T}$, and $U_\partial = k\sqrt{U}$.

A key distinction emerges between the behavior of the model with bulk interactions, as formulated in Eqs. (9), and that incorporating

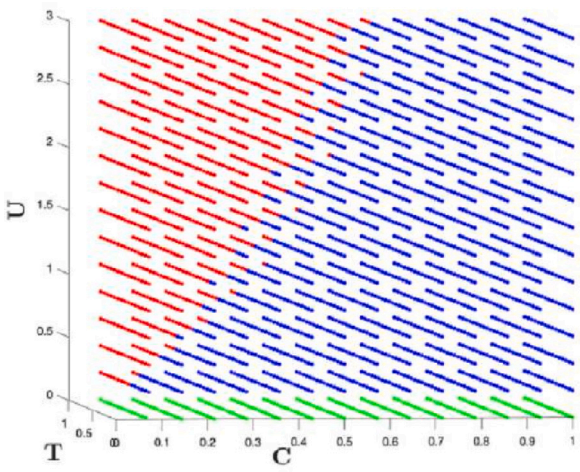

Fig. 3. The phase space of the system (8) with the parameters set as in the scenario Σ_1 of Table 2, with the attraction basins of the three dynamical structures highlighted: red dots are initial conditions ending in the E_1 of Fig. 1; the green dots are initial condition ending in the E_2 point of the same figure; the initial conditions converging to the limit cycle are represented with blue dots.

border interactions, described by Eqs. (8). As thoroughly discussed in Section 3.2, the choice to model certain interactions as boundary-driven rather than bulk-mediated leads to qualitatively different predictions. Notably, the phase space associated with the border interaction model exhibits a greater diversity of dynamical scenarios (in particular, the border interaction model predicts the existence of a limit cycle), suggesting that spatial edge effects play a critical role in shaping ecological outcomes.

Once the border interaction paradigm is adopted, the system in which *Cystoseira s.l.*, turf, and sea urchin populations are treated as dynamical variables corresponds to Eqs. (8). This system involves several parameters, and varying them yields a diverse set of dynamical behaviors. We have hence explored the range of ecological scenarios that emerge from these parameter choices, through both numerical simulations and analytical insights when feasible. The full system reveals an even richer phase space, admitting scenarios with asymptotic equilibria involving extinctions, as well as limit cycles. It may also exhibit a unique equilibrium where all three populations – C, T, and U – persist at nonzero, steady-state levels.

Comparing the predictions of our model with real-world observations is not straightforward, owing to the experimental challenges outlined in Introduction. Nonetheless, we reference two empirical studies whose findings can be loosely compared with the behavior exhibited by our model.

The first study, reported in Humphries et al. (2020), provides a quantitative assessment of the role of sea urchin grazing, demonstrating that its contribution to controlling algal abundance can be as significant as that of herbivorous fish. In our model, the presence of sea urchins plays a pivotal role in regulating algal dynamics, leading to equilibrium configurations that would not arise in their absence – for example, the emergence of the stable equilibrium E_0 in scenario Σ_2 of Table 2. Furthermore, the reciprocal influence of algae on sea urchin dynamics proves to be essential, as evidenced by the differing outcomes between the constant-U (see Appendix C) and fully coupled versions of the model.

The second study we want to mention to compare with our model is Palacìn et al. (1998), in which the impact of sea urchins on frondose and turfing algae in the Western Mediterranean is shown to be relevant even when the sea urchin density is low. Figure 2 of Palacìn et al. (1998) suggests that sea urchin grazing has a stronger impact on turf-forming algae than on canopy-forming species. When sea urchins are reintroduced into areas from which they had previously been removed, the coverage of frondose algae remains broadly comparable to that in both the control sites and the urchin-free regions. In contrast, turfing algae exhibit a marked decline relative to the grazer-free condition. This result may stem from the fact that sea urchins can graze across the entire turf area, whereas only the edges of canopy patches are accessible to them – an asymmetry that our model is specifically designed to capture and quantify.

Our investigation into the significance of border effects thus appears to be well-founded, as border interactions play a critical role in marine ecosystem dynamics. Patterns observed in real-world marine ecosystems that do not match the typical population dynamics generally used in ecological models – specifically, interactions among competing species that do not involve all individuals in the same way – may alter the outcome of the overall ecological dynamics. This may have important implications for conservation and restoration actions, and contribute to explaining the difficulties observed both in natural recovery and in assisted re-colonization of degraded habitats by *Cystoseira s.l.* communities (Bonaviri et al., 2011; Tamburello et al., 2019b; Cebrian et al., 2021; Bernal-Ibáñez et al., 2024).

Our ecological model can be employed in calibrations with experimental data: a realistic, evidence-based, context-specific choice of parameters will make the model applicable to the adaptive management of the ecosystem for which it has been calibrated. To this end, the model could be further complicated, for instance by adding a fish population variable F describing predators of sea urchins. One could then tune the fish population mortality taking into account fishing intensity, and investigate the impact of anthropic harvesting pressure on the system (this would be more realistic than encoding the effect of fishing in a modification of the sea urchin mortality Δ_U).

Before concluding our discussion, it is worth outlining a few potential developments of the current model and the conceptual framework it embodies.

An interesting avenue for future research would be to develop an economic model layered atop the ecological system governed by Eqs. (8) in order to assess how the presence of stand-alone dynamics for the resource C – notably involving $\sqrt{C}$ terms rather than the standard logistic formulation – alters the estimated value of coastal ecosystem services.

As discussed in detail in Appendix A.4, our topological reasoning leads to the assumption that the relationship between border and bulk population reads $X_\partial = k\sqrt{X}$ due to the 2-dimensional nature of the sea bed. This can be applied to the case in which the small scale complexity of the rocky bottom is low. In contrast, when the topographic complexity of the bottom is high (e.g., presence of boulders, pits, holes or crevices), the sea floor would appear as a "fat fractal", with real dimension $\nu > 2$ (a "fat fractal" is said to have a Hausdorff dimension larger than the space that *apparently* contains it). The use of fractal dimension of the seafloor as a characteristic of its potential biodiversity is well reported in the literature, see e.g. Connell et al. (2014). As a consequence, one could argue $X_\partial = kX^\delta$, being $\delta \simeq \frac{\nu-1}{\nu} \in \mathbb{R}$, and the equations in (8) would be replaced by equations where terms with fractional powers replace the square roots (as in certain epidemiological models, see e.g. Materassi (2019)).

The inclusion of boundary interactions is a relevant, intrinsic feature of our model, not intended to reflect any specific spatial or temporal scale, nor designed to target a particular ecological question. Still, the question of whether there are conditions in which the use of border effects is not strictly necessary may make sense. Future analyses of the just mentioned extension of the model with $X_\partial = kX^\delta$ and $\delta \in (0, 1]$ (that is out of the scope of this paper) will show the regimes for which different δs (e.g., $\delta = 1$ and $\delta = \frac{1}{2}$) yield similar results. This will also highlight the conditions under which a bulk interaction model is grossly equivalent to the more sophisticated border interaction one.

Finally, we note that the same trophic web could also be effectively described using alternative mathematical frameworks, such as

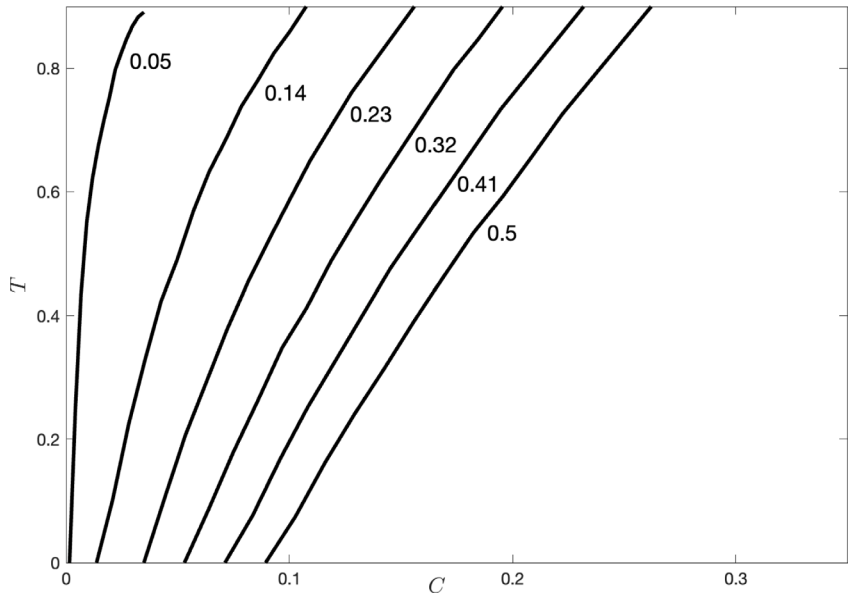

Fig. 4. Regions of attraction in the CT-plane for values of U ranging from 0.05 to 0.5. Each line, corresponding to the U-value indicated beside it, divides the plane into a left-upper part, where trajectories are attracted by the equilibrium E_1, and a right-lower part, where trajectories are attracted by the limit cycle (such as the trajectory of Fig. 2). For $U = 0$ (not represented in the plot) all initial states with $C > 0$ are attracted by E_2 and initial data with $C = 0$ are attracted by E_1.

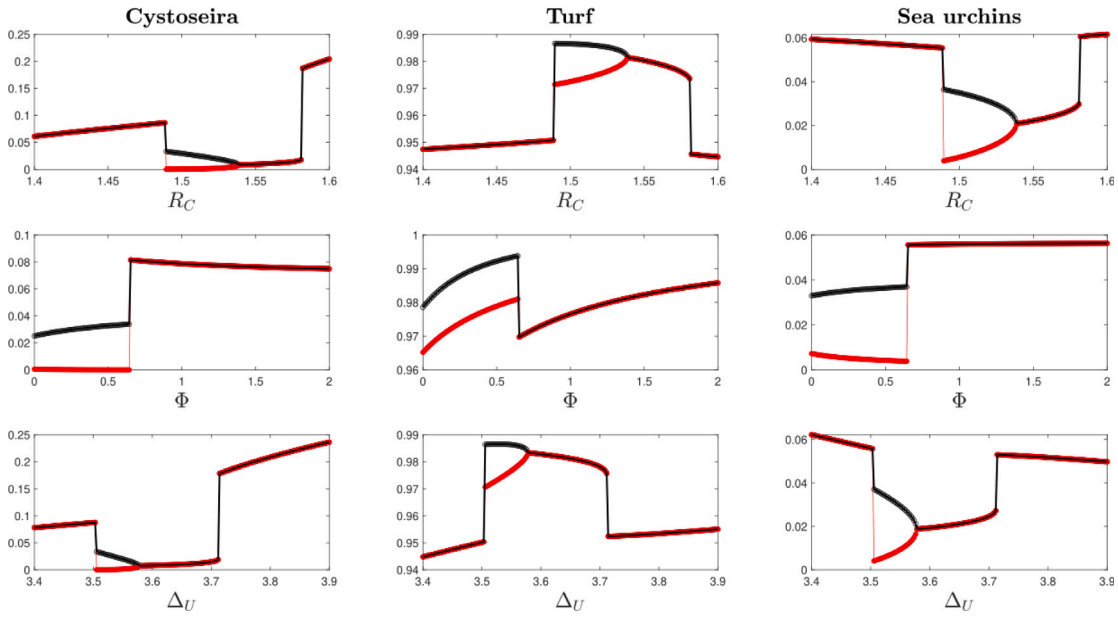

Fig. 5. Bifurcation study for the system (8) depending on R_C, Φ and Δ_U: all the parameters not appearing in the single specific plot are set as in the scenario Σ_1 in Table 2. From top to bottom: bifurcation as depending on the *Cystoseira s.l.* stand-alone growth rate R_C, the turf-exogenous growth rate Φ, and the sea urchin mortality rate Δ_U, while keeping the other two parameters fixed. Black and red lines denote, respectively, the asymptotic maximum and minimum of the trajectory. The two values coincide for a point attractor and differentiate for a cycle attractor (stable limit cycle). As the plots were constructed by running the numerical simulations for the dynamics, only stable critical loci may be found.

space-explicit models based on partial differential equations (PDEs), in which dynamical variables are replaced by spatial fields representing local population densities. These PDE formulations serve as mean-field approximations of individual-based models (IBMs), where *Cystoseira s.l.*, turf, and sea urchins are treated as autonomous agents operating according to species-specific ecological rules. For example, in such an IBM, only the individuals of *Cystoseira s.l.* located along the canopy edge at time step t would generate new individuals at time $t + 1$. The application of space-explicit approaches is expected to reveal emergent spatial patterns on the seafloor, enabling comparison with observed configurations in natural ecosystems. These extensions will be the focus of future research.

CRediT authorship contribution statement

D. Collini: Investigation, Formal analysis, Data curation, Conceptualization. **L. Barletti:** Methodology, Investigation, Conceptualization. **F. Bulleri:** Writing – review & editing, Investigation, Conceptualization. **S. Dalmazzone:** Visualization, Formal analysis, Conceptualization. **V.**

Frontuto: Writing – review & editing, Writing – original draft, Visualization, Formal analysis. **L. Tamburello:** Writing – review & editing, Writing – original draft, Visualization, Supervision, Investigation, Conceptualization. **F. Sarnari:** Validation, Software, Formal analysis. **M. Materassi:** Writing – review & editing, Writing – original draft, Investigation, Formal analysis, Conceptualization.

Declaration of competing interest

The authors declare that they have no known competing financial interests or personal relationships that could have appeared to influence the work reported in this paper.

Acknowledgment

The work of M. Materassi was partially supported by the Project *The structure, dynamics and control of network systems with higher-order interactions*, contract number 2022FHHHPC of the Italian Ministry of University and Research.

The Authors would like to warmly acknowledge the memory of Professor Ezio Venturino of the University of Turin (Italy), who passed away in May 2025. He brought to our attention the work in the Ref. Ajraldi et al. (2011), deeply inspiring our theoretical construction.

Appendix A. Mathematical construction of the model

In the present Appendix, the model equations are constructed step-by-step, with all the details that were necessarily omitted in the presentation of the model in Methods. All the conventions and symbols introduced in Methods do hold here, see e.g. the meaning of the many parameters reported in Table 1.

A.1. Processes modeled and simplifying hypotheses

The model is constructed considering each different process taking place in the trophic web.

Let us first consider *algal recruitment*.

Cystoseira s.l. and turf algae show different diffusion mechanisms. Propagules of *Cystoseira s.l.* generally have limited dispersal, settling within few meters from the mother alga (Mangialajo et al., 2012; Thibaut et al., 2014). When these propagules fall within the canopy bulk, the shadowing of adult algae renders their probability to survive very small (Wernberg, 2008; Piazzi et al., 2017). As a consequence, not all the C individuals take part in the recruitment with the same probability of success as the C_∂ border ones: these algae are the individuals most effectively reproducing. The drastic simplification adopted here is that C_∂ is the only part of the population C involved in recruitment.

Turf algae show a double recruitment mechanism. Local recruitment takes place involving the sole border individuals T_∂ out of T, that successfully recruit right outside the turf mat: here, the same approximation of *Cystoseira s.l.* applies; moreover, a rain of turf propagules carried by sea currents gives rise to a recruitment term proportional to some constant flux Φ, considered time-independent as *seasonal effects are neglected*.

The first inter-algal competition mechanism is *shadowing*: *Cystoseira s.l.* fronds shadow the turf algae living as canopy undergrowth, while turf algae, growing on *Cystoseira s.l.* fronds as epiphytes, partially shield the light hitting the Fucales. To our best knowledge, this is the first time that such an effect is put into a closed mathematical form.

The other competition mechanism is *border competition*: *Cystoseira s.l.* propagules falling in a thick turf region have a low probability of surviving. The chances of survival substantially increase if C propagules fall where the rocky bed is only partially populated by turf-forming algae. Instead, propagules of some turf algal species easily survive in the canopy, living as epiphytes or as undergrowth (Ballesteros et al., 1998). The low probability of *Cystoseira s.l.* propagules to survive within the turf carpet yields a net cost given by competition between C_∂ and T_∂ along the canopy-turf border into the C dynamics. No such cost term appears in the turf evolution equation, as turf propagules may survive within the canopy.

The next ecological process modeled is *sea urchin grazing*. Due to the morphological differences between the arborescent algae and the short turf, sea urchins graze the two groups in different ways. Sea urchins simply graze the turf carpet all over the place, meeting little resistance to their movement. This involves all T and all U in the turf-grazing terms of the model equations. Grazing *Cystoseira s.l.* is more complicated as it forms a rather solid barrier, difficult to penetrate for sea urchins. Moreover, the fronds of *Cystoseira s.l.* moved by sea currents act as a whip on sea urchins, keeping them at a distance (Agnetta et al., 2013). Sea urchins thus mostly browse the canopy along its border: in the model this fact is approximated by assuming that only the border individuals C_∂ and U_∂ are involved in the grazing of *Cystoseira s.l.* (note that, in principle, all the U sea urchins might take part in grazing the C_∂ algae, but we consider that these invertebrates have a very scarce mobility, so one does not expect that sea urchins come from afar, i.e. from the bulk of the sea urchin pack, to graze the canopy border within a useful time).

Processes involving border interactions break one of the most important assumptions generally used to represent population dynamics in ecological models, i.e. the so-called *law of mass action* (Érdi and Tóth, 1989; May, 1974; House, 2012; Materassi, 2019; Fanelli and Piazza, 2020). This law states that all individuals within a population are identical in taking part in predation, growth, and recruitment. Here, instead, only the community border individuals take part in *Cystoseira s.l.* recruitment, turf endogenous recruitment, *Cystoseira*-turf border competition, and *Cystoseira s.l.* grazing by sea urchins (equivalently, one may state that the law of mass action is applied to the subpopulations C_∂, T_∂ and U_∂ in the case of border interactions).

In order to write the dynamics of the model, one has to find a closed expression of the relationship between a total population X, living in a region $\mathbb{D}$ of the seabed, and the portion X_∂ of it located on its border $\partial\mathbb{D}$. The solution chosen to express X_∂ in terms of X is inspired by *herd behavior* in the mathematical ecology of animals (Ajraldi et al., 2011): for animals that move in impenetrable packs, only the portion of individuals located on the border of the pack interacts with other species. Here we express $C_\partial(C)$, $T_\partial(T)$ and $U_\partial(U)$ in the same way animal ecology selects the pack-border population out of the total one, see Appendix A.2: the key relationship expressing $X_\partial(X)$ is Eq. (A.15) below.

According to all the aforementioned ecological facts, a set of ODEs are written for (C,T,U), and the consequent phase space structure of the flux $\left(\frac{dC}{dt},\frac{dT}{dt},\frac{dU}{dt}\right)$ is studied.

In order to put together the aforementioned processes, taking into account the hypotheses mentioned, the dynamics of a generic population X is written as

$$\frac{dX}{dt} = V^X_{\rm rec} + V^X_{\rm cons} + V^X_{\rm int} : \tag{A.1}$$

$V^X_{\rm rec} \geq 0$ is the recruitment term through which X increases, $V^X_{\rm cons} \leq 0$ is the consumption term due to which X decreases, and $V^X_{\rm int}$ is the sum of all terms describing interactions between X and another species without biomass transfer (hence, predation/grazing and natural mortality are included in $V^X_{\rm cons}$, whereas $V^X_{\rm int}$ includes competition or cooperation terms). Note that in the case of the *Cystoseira*-turf system, the recruitment terms are modulated by some non-mass-transferring interactions, namely shadowing factors, see below, so that the separation of the two addenda $V^X_{\rm rec}$ and $V^X_{\rm int}$ does not represent the mathematics exhaustively, as thoroughly explained in what follows (rigorously speaking, despite its very small number of nodes, this system (C,T,U) is a typical example of network with "higher order interactions", see for instance Boccaletti et al. (2023), where the link between two nodes involves the state of some other node).

We are particularly interested in the co-existence of the species, i.e. in the presence of attractive pointlike or extended structures in which none of the three variables C, T and U vanishes. Ecological resilience may be thought of as the size of the basin of attraction of such biodiversity-rich structures, or the magnitude of disturbance that can be absorbed before the system converges to a different state (Holling, 1973; Andersen et al., 2009; Rocha et al., 2015; Gunderson, 2000).

The form (A.1) for the ODEs of the state (C,T,U) yields the system:

$$\begin{cases} \dfrac{dC}{dt} = V^C_{\text{rec}}(C,T) + V^C_{\text{cons}}(C,U) + V^C_{\text{int}}(C,T), \\ \dfrac{dT}{dt} = V^T_{\text{rec}}(T,C) + V^T_{\text{cons}}(T,U) + V^T_{\text{int}}(T,C), \\ \dfrac{dU}{dt} = V^U_{\text{rec}}(U,C,T) + V^U_{\text{cons}}(U,\ldots) \end{cases} \tag{A.2}$$

(the shadowing contribution is encoded in the fact that the V^C_{rec} and the V^T_{rec} depend on the other algal variable too; the meaning of ellipsis in V^U_{cons} is explained below). In Eqs. (A.2) it is evident that C and T compete with each other, while U graze them both.

A.2. The role of border individuals

In order to write the recruitment term of *Cystoseira s.l.* as V^C_{rec}, one has to take into account the processes promoting such recruitment and those limiting it: in particular, since the success of *Cystoseira s.l.* propagules can be limited by the action of turf algae as shielding epiphytes, we state that this term depends both on C and T as $V^C_{\text{rec}} = V^C_{\text{rec}}(C,T)$, with the condition $\frac{\partial V^C_{\text{rec}}}{\partial T} < 0$ (the more abundant the turf, the less effective the C recruitment). Similarly, also the turf recruitment term $V^T_{\text{rec}} = V^T_{\text{rec}}(T,C)$ depends on the population *Cystoseira s.l.*, since the shadowing by *Cystoseira s.l.* limits the growth of turf, with the condition $\frac{\partial V^T_{\text{rec}}}{\partial C} < 0$ (the more abundant the Fucales, the more shadowed, i.e. limited in its development, the turf).

Since the *Cystoseira s.l.* individuals taking part in the recruitment process are only those on the border of the canopy, $V^C_{\text{rec}}(C,T)$ should be re-written as $V^C_{\text{rec}}(C,T) = \upsilon^C_{\text{rec}}(C_\partial,T)$ (one should understand $V^C_{\text{rec}}(C,T) = \upsilon^C_{\text{rec}}(C_\partial(C),T)$, as the border amount C_∂ will be expressed as depending on the total C in Appendix A.4 below).

As far as turf recruitment is concerned, we have mentioned that two processes are at work: (i) an exogenous term $\upsilon^{\text{exo}}_{\text{rec}}(T,C)$, so that $\frac{\partial \upsilon^{\text{exo}}_{\text{rec}}}{\partial C} < 0$ due to shadowing competition; and (ii) an endogenous term $\upsilon^{\text{en}}_{\text{rec}}(T_\partial,C)$, due to vegetative growth, working exactly as the recruitment of *Cystoseira s.l.*, in which only the border turf individuals appear (here C mimics the shadowing effect of *Cystoseira s.l.* individuals on turf, so that also $\frac{\partial \upsilon^{\text{en}}_{\text{rec}}}{\partial C} < 0$ holds). All in all, one has: $V^T_{\text{rec}}(T,C) = \upsilon^{\text{exo}}_{\text{rec}}(T,C) + \upsilon^{\text{en}}_{\text{rec}}(T_\partial,C) \geq 0$.

The consumption terms $V^C_{\text{cons}}(C,U)$ and $V^T_{\text{cons}}(T,U)$ represent the decrement of algal biomass due to the grazing by sea urchins, needing to encode that sea urchins graze at the border of the *Cystoseira s.l.* canopy while turf is grazed everywhere. In $V^C_{\text{cons}}(C,U)$ the individuals taking part in the process are those meeting at the intersection of the borders of the canopy and sea urchin regions, so that one has $V^C_{\text{cons}}(C,U) = \upsilon^C_{\text{cons}}(C_\partial,U_\partial) \leq 0$. Instead, as all the individuals of the turf populations may be grazed by all individuals of the sea urchin population, the turf consumption term depends on T and U directly, as $V^T_{\text{cons}}(T,U) \leq 0$.

The interaction terms $V^C_{\text{int}}(C,T)$ and $V^T_{\text{int}}(T,C)$ represent the competition between *Cystoseira s.l.* and turf populations, other than the shadowing competition. We have assumed that *Cystoseira s.l.* propagules falling in the turf region have serious difficulties growing, while turf propagules may survive and grow in the *Cystoseira s.l.* canopy. As a result of this asymmetry, we approximate $V^T_{\text{int}}(T,C) = 0$ in the model, while the interaction hindering the growth of *Cystoseira s.l.* propagules falling in the turf region will involve only the C_∂ individuals producing them and the T_∂ individuals meeting them, that is: $V^C_{\text{int}}(C,T) = \upsilon^C_{\text{int}}(C_\partial,T_\partial) \leq 0$.

In the model, the recruitment of sea urchins is simply the population growth obtained through the consumption of algae. Thus, the term $V^U_{\text{rec}} \geq 0$ is written as

$$V^U_{\text{rec}}(U,C,T) = -c_{CU}\upsilon^C_{\text{cons}}(C_\partial,U_\partial) - c_{TU}V^T_{\text{cons}}(T,U),$$

where the sign takes into account that, in the grazing process, the recruitment of sea urchins corresponds to a decrease in algal populations (indeed, the terms $\upsilon^C_{\text{cons}}(C_\partial,U_\partial)$ and $V^T_{\text{cons}}(T,U)$ are semi-negative defined), while c_{CU} and c_{TU} are positive metabolic factors.

The last term in the third ODE in (A.2) is the decrease in the sea urchin population $V^U_{\text{cons}}(U,\ldots)$ by predation or natural mortality. The ellipsis is for the possible involvement of other species feeding on sea urchins, e.g. fish such as Sparids. In our model, no populations other than C, T and U are involved, so the only consumption term for U is the natural death of a heterotrophic population, i.e. $V^U_{\text{cons}}(U) = -\Delta_U U$, being $\Delta_U > 0$ the inverse of the average time of survival to starvation (the characteristic time of exponential decrease of $U(t)$ with time in the absence of any other population). Variations in predation pressure on sea urchins may be accounted for by tuning Δ_U.

All in all, the system of ODEs is re-written as

$$\begin{cases} \dfrac{dC}{dt} = \upsilon^C_{\text{rec}}(C_\partial,T) + \upsilon^C_{\text{cons}}(C_\partial,U_\partial) + \upsilon^C_{\text{int}}(C_\partial,T_\partial), \\ \dfrac{dT}{dt} = \upsilon^{\text{exo}}_{\text{rec}}(T,C) + \upsilon^{\text{en}}_{\text{rec}}(T_\partial,C) + V^T_{\text{cons}}(T,U), \\ \dfrac{dU}{dt} = -c_{CU}\upsilon^C_{\text{cons}}(C_\partial,U_\partial) - c_{TU}V^T_{\text{cons}}(T,U) - \Delta_U U. \end{cases} \tag{A.3}$$

A.3. Shadowing factors and grazing

The algae are autotrophic organisms, requiring resources available on the sea floor (i.e., nutrients from the water column, space and light). According to this, a possible mathematical expression for the recruitment terms for them is a logistic form, taking into account the growth rate due to sunlight and nutrients, and a suitable carrying capacity based on the environmental resources available. Let the carrying capacities for the two species be K_C and K_T, so that the recruitment terms can be written as:

$$\begin{aligned} \upsilon^C_{\text{rec}}(C_\partial,T) &= \xi(T)R_C C_\partial\left(1 - \frac{C_\partial}{K^\partial_C}\right), \\ \upsilon^{\text{exo}}_{\text{rec}}(T,C) &= \eta(C)\Phi\left(1 - \frac{T}{K_T}\right), \\ \upsilon^{\text{en}}_{\text{rec}}(T_\partial,C) &= \rho(C)R_T T_\partial\left(1 - \frac{T_\partial}{K^\partial_C}\right), \end{aligned} \tag{A.4}$$

$$\xi,\ \eta,\ \rho \in (0,1],\ \frac{d\xi}{dT} \leq 0,\ \frac{d\eta}{dC} \leq 0,\ \frac{d\rho}{dC} \leq 0.$$

The carrying capacities $K^\partial_{C,T}$ are those relative to the populations C_∂ and T_∂, that we will quantify in a while.

As the only growth term of *Cystoseira s.l.* is the logistic one involving the border of the canopy, this means that, if C were chosen to represent the total population of the canopy, its growth is supposed to be due only to the appearance of new individuals, produced by the C_∂ border ones, and not by the growth of all the algae, that are instead assumed to have and maintain all the same mass, equal to some average value: this reasoning holds if C, T and U are considered as biomass variables. The pre-factors ξ, η and ρ in (A.4) take into account the shadowing competition between the two macroalgal groups, which reduces the effective growth rates. ξ is the light attenuation on the *Cystoseira s.l.*

branches due to the epiphytic turf; η represents the shadowing of the *Cystoseira s.l.* on the turf undergrowth in the canopy; ρ is the shadowing factor of the *Cystoseira s.l.* on the turf propagules falling right outside the turf region: in the present model, we assume $\rho = 1$, i.e. we neglect for simplicity the border shadowing effect of *Cystoseira s.l.* on turf algae. As the rival alga population grows, the shadowing factors reduce the growth rate of the population at hand more and more: in general, one has no shadowing for zero rival population, so that $\xi(0) = 1$ and $\eta(0) = 1$, while when the rival population is maximum the recruitment terms reach their minimum value: if the carrying capacities K_C and K_T represent the natural maxima reached by C and T, one assumes $\xi(K_T) = \xi_{\min}$ and $\eta(K_C) = \eta_{\min}$ represent the minimum value of ξ and η.

Two alternative mathematical forms of shadowing factors can be used: either exponential

$$\xi(T) = e^{-\frac{T}{T_0}},\ \eta(C) = e^{-\frac{C}{C_0}},\ T_0 = -\frac{K_T}{\ln \xi_{\min}},\ C_0 = -\frac{K_C}{\ln \eta_{\min}} \tag{A.5}$$

or algebraic

$$\xi(T) = 1 - \frac{T}{T_0^*},\ \eta(C) = 1 - \frac{C}{C_0^*},\ T_0^* = \frac{K_T}{1-\xi_{\min}},\ T < T_0^*,$$
$$C_0^* = \frac{K_C}{1-\eta_{\min}}\ C < C_0^* \tag{A.6}$$

(in general one has $C_0^* \neq C_0$ and $T_0^* \neq T_0$, even if (A.6) could be understood as the first order Taylor expansion of (A.5)). Both the definitions (A.5) and (A.6) fulfill the mathematical requirements for ξ and η in (A.4): the best choice between them is matter of modeling opportunity.

Whereas the local recruitment terms $v_{\text{rec}}^{C}(C_\partial, T)$ and $v_{\text{rec}}^{\text{in}}(T_\partial, C)$ are linear in the populations involved, as $R_C C_\partial$ and $R_T T_\partial$ respectively, in the exogenous recruitment term $v_{\text{rec}}^{\text{exo}}(T, C)$ a constant factor Φ mimics the population-independent exogenous flux of turf propagules. This means

$$v_{\text{rec}}^{C}(0,T) = 0,\ v_{\text{rec}}^{\text{en}}(0,C) = 0,\ v_{\text{rec}}^{\text{exo}}(0,C) \neq 0\ :$$

even if the *local* population of turf vanishes, a *local* re-growth of T still takes place, due to the *non-local* contribution of turf propagules coming from afar, brought by sea currents.

The interaction term $v_{\text{int}}^{C}(C_\partial, T_\partial)$ is written as a rather traditional competition term $v_{\text{int}}^{C}(C_\partial, T_\partial) = -\beta C_\partial T_\partial$, with $\beta > 0$: choosing β suitably, we can represent the situation according to which *Cystoseira s.l.* propagules may survive in a region partially populated by a thin turf, rather than stating crudely that *Cystoseira s.l.* propagules do not survive at all in the turf.

Finally, let us discuss the terms of consumption of algae by sea urchins, i.e. the addenda $v_{\text{cons}}^{C}(C_\partial, U_\partial)$ and $V_{\text{cons}}^{T}(T, U)$. Two possible options are mentioned here, considering the sea urchins either *insatiable*, or *satiable*, i.e. either letting the *per capita* grazing rate grow indefinitely with the alga abundance, or have a saturation, respectively. In the first case, one writes:

$$v_{\text{cons}}^{C}(C_\partial, U_\partial) = -a_{CU} C_\partial U_\partial,\ V_{\text{cons}}^{T}(T,U) = -a_{TU} TU, \tag{A.7}$$

namely Holling Type I response function, while in the second case, one may use the form:

$$v_{\text{cons}}^{C}(C_\partial, U_\partial) = -\frac{A_{CU} C_\partial U_\partial}{B_{CU} + C_\partial},\ V_{\text{cons}}^{T}(T,U) = -\frac{A_{TU} TU}{B_{TU} + T}, \tag{A.8}$$

namely Holling Type II response function. In this second, more realistic case of satiable sea urchins, the ODEs are written as:

$$\begin{cases} \dfrac{dC}{dt} = \xi(T) R_C C_\partial \left(1 - \dfrac{C_\partial}{K_C^\partial}\right) - \beta C_\partial T_\partial - \dfrac{A_{CU} C_\partial U_\partial}{B_{CU} + C_\partial}, \\ \dfrac{dT}{dt} = \eta(C) \Phi \left(1 - \dfrac{T}{K_T}\right) + R_T T_\partial \left(1 - \dfrac{T_\partial}{K_T^\partial}\right) - \dfrac{A_{TU} TU}{B_{TU} + T}, \\ \dfrac{dU}{dt} = -c_{CU} \dfrac{A_{CU} C_\partial U_\partial}{B_{CU} + C_\partial} - c_{TU} \dfrac{A_{TU} TU}{B_{TU} + T} - \Delta_U U. \end{cases} \tag{A.9}$$

The same system for insatiable sea urchins, less realistic, is obtained by using the terms in (A.7).

About the second ODE in (A.9), $\frac{dT}{dt} = \cdots$, one should stress that, depending on the species forming the turf, the term $v_{\text{rec}}^{\text{en}} = R_T T_\partial \left(1 - \frac{T_\partial}{K_T^\partial}\right)$ of local (endogenous) recruitment may be the prevalent one. Different biodiversity conditions in the turf species community may be selected by choosing Φ, R_T and K_T suitably.

A.4. Calculating $C_\partial(C)$, $T_\partial(T)$ and $U_\partial(U)$

Writing the Eqs. (A.9) in a closed form requires expressing the subpopulations X_∂ in terms of the populations X, for $X = C, T, U$. For this, we take inspiration from the mathematics of *herd behavior* in animal ecology (Ajraldi et al., 2011).

In order to obtain the expression $X_\partial(X)$, let us suppose that these individuals are located all over an environment $\mathbb{E}$ of dimension n:

$$\dim \mathbb{E} = n. \tag{A.10}$$

The statement (A.10) may be understood in different ways: we can give it a strictly algebraic sense, as $\mathbb{E} = \mathbb{R}^n$, or a more general one if $n \notin \mathbb{N}$, and $n \in \mathbb{R}^+$, as in some study on epidemic outbreaks (Materassi, 2019). If a finite region $\mathbb{D}$ of linear "size" ℓ is considered within $\mathbb{E}$

$$\mathbb{D} \subset \mathbb{E},\ \ell(\mathbb{D}) \overset{\text{def}}{=} \langle d_{\mathbb{E}}(\boldsymbol{x}, \boldsymbol{y}) \rangle_{\mathbb{D}}\ /\ \boldsymbol{x}, \boldsymbol{y} \in \mathbb{D}, \tag{A.11}$$

the "measure" of the region $\mathbb{D}$ has the property

$$\mu(\mathbb{D}) = \mathbb{O}(\ell^n), \tag{A.12}$$

where the symbol $\mathbb{O}(\ell^n)$ means *grows with ℓ as its nth power ℓ^n* (the statements in (A.11) require the ambient $\mathbb{E}$ to be equipped with a metric structure $d_{\mathbb{E}}$, while $\langle\cdot\rangle_{\mathbb{D}}$ means "average over the points in $\mathbb{D}$"; Eq. (A.12) also implies the definition of a measure μ on $\mathbb{E}$: all in all, one should state $\mathbb{E}$ to be a *topological, metric space with a measure on it*).

In a space-implicit model of the trophic web, one imagines the populations as homogeneously distributed in the regions of interest within $\mathbb{E}$, so that one can figure the number of individuals in a population X contained in $\mathbb{D}$, or their total biomass, to be simply proportional to the measure $\mu(\mathbb{D})$:

$$X(\mathbb{D}) \propto \mu(\mathbb{D}) \implies X(\mathbb{D}) = \mathbb{O}(\ell^n) \tag{A.13}$$

(the symbol "$\propto$" means "proportional to").

Consider now the part of the population X that is located on the border $\partial\mathbb{D}$ of the region $\mathbb{D}$: if the domain $\mathbb{D}$ is "regular enough", one expects:

$$\mu(\mathbb{D}) = \mathbb{O}(\ell^n),\ \mu(\partial\mathbb{D}) = \mathbb{O}\left(\ell^{n-1}\right) \tag{A.14}$$

(here we use the same symbol μ for the measure of $\mathbb{D}$ and for that of $\partial\mathbb{D}$, even if they could be different concepts, e.g. $\mu(\mathbb{D})$ being a volume and $\mu(\partial\mathbb{D})$ a surface). All in all, a consequence of the space-implicit model assumptions determining $\ell = \mathbb{O}\left(X^{\frac{1}{n}}\right)$, from (A.13) and (A.14) one may conclude:

$$X_\partial = \mathbb{O}\left(X^{\frac{n-1}{n}}\right). \tag{A.15}$$

This is the central relationship on which our model is based.

As the populations of *Cystoseira s.l.* C, of turf T and of sea urchins U live within the 2-dimensional environment of the seafloor, the case of interest in this work is $n = 2$, so that from (A.15) one has

$$X_\partial = \mathbb{O}\left(\sqrt{X}\right). \tag{A.16}$$

The two carrying capacities relative to border populations may be expressed simply as $K_C^\partial = \sqrt{K_C}$ and $K_T^\partial = \sqrt{K_T}$, as explained in Appendix B with some detail. This allows us to construct the ODEs for the 3-trophic system, implementing the biological conditions described before, in the forms of the system (8), and the two "reduced" ones (C.1) and (C.2) described in Appendix C.

Appendix B. Border populations, square roots and coefficient units

The use of the square root of the populations $\sqrt{C}$, $\sqrt{T}$ and $\sqrt{U}$ in the system (3), and its more explicit version (8) where the form of the response function has been chosen, is motivated by the assumption

$$X_\partial = k_n \sqrt{m_x X}, \tag{B.1}$$

as obtained in Methods. Based on this (B.1), it is easy to show that all the expressions in (8) involving X_∂ are correct, provided the coefficients of the model are defined suitably, so to include properly the form factors k_n and k as anticipated.

Starting with the "stand alone" growth term of *Cystoseira s.l.*, and the endogenous border growth of turf, provided only C_∂ and T_∂ contribute as

$$\left(\frac{dC}{dt}\right)_0 = R_C^\partial C_\partial \left(1 - \frac{C_\partial}{K_C^\partial}\right), \quad \left(\frac{dT}{dt}\right)_0 = R_T^\partial T_\partial \left(1 - \frac{T_\partial}{K_T^\partial}\right),$$

one may use (B.1) and obtain:

$$\begin{aligned}\left(\frac{dC}{dt}\right)_0 &= R_C^\partial k_n \sqrt{m_C C}\left(1 - \frac{k_n\sqrt{m_C C}}{K_C^\partial}\right), \quad \left(\frac{dT}{dt}\right)_0 \\ &= R_T^\partial k_n \sqrt{m_T T}\left(1 - \frac{k_n\sqrt{m_T T}}{K_T^\partial}\right).\end{aligned} \tag{B.2}$$

Then, it is rather obvious that, if the relationship (B.1) inspires

$$R_{C,T}^{\surd} \overset{\text{def}}{=} R_{C,T}^\partial k_n \sqrt{m_{C,T}}, \quad K_{C,T}^\partial \overset{\text{def}}{=} k_n \sqrt{m_{C,T} K_{C,T}^{\surd}}, \tag{B.3}$$

the two stand-along recruitment terms (B.2) may take the form

$$\left(\frac{dC}{dt}\right)_0 = R_C^{\surd}\sqrt{C}\left(1 - \frac{\sqrt{C}}{\sqrt{K_C^{\surd}}}\right), \quad \left(\frac{dT}{dt}\right)_0 = R_T^{\surd}\sqrt{T}\left(1 - \frac{\sqrt{T}}{\sqrt{K_T^{\surd}}}\right): \tag{B.4}$$

the parameters $R_{C,T}^{\surd}$ and $K_{C,T}^{\surd}$ are precisely those concisely indicated as $R_{C,T}$ and $K_{C,T}$ in (8). The passages (B.3) and (B.4) are simply useful to justify the use of the square root of populations in stand-alone logistic terms $\left(\frac{dC}{dt}\right)_0$ and $\left(\frac{dT}{dt}\right)_0$. If the identification of $R_{C,T}$ and $K_{C,T}$ respectively with $R_{C,T}^{\surd}$ and $K_{C,T}^{\surd}$ is done in (8), the nature of these coefficients in terms of biophysical quantities is the following:

$$\text{(B.3)} \implies [R_{C,T}]_{(8)} = \frac{\sqrt{\text{m}}}{\text{t}}, \quad [K_{C,T}]_{(8)} = \text{m}, \tag{B.5}$$

where "t" means "dimensionally time" and "m" is "dimensionally biomass", being $[q]$ the dimensional expression of the physical quantity q.

In the system (8), the same reasoning can be applied to the coefficient β, quantifying the border competition between canopy and turf: if the limiting term for the *Cystoseira s.l.* is

$$\left(\frac{dC}{dt}\right)_\beta = -\beta_\partial C_\partial T_\partial = -\beta_\partial k_n^2 \sqrt{m_C m_T C T},$$

implying the dimensional equation $[\beta^\partial] = \frac{1}{\text{m t}}$, one may define

$$\beta^{\surd} = \beta_\partial k_n^2 \sqrt{m_C m_T}, \tag{B.6}$$

so that the limiting term due to border competition reads

$$\left(\frac{dC}{dt}\right)_\beta = -\beta^{\surd}\sqrt{CT}.$$

This $\beta^{\surd}$ is the same parameter indicated as β in (8). From (B.6) one easily obtains the corresponding dimensional equation for the coefficient named β in (8), our $\beta^{\surd}$ here, that is:

$$\text{(B.3)} \implies [\beta]_{(8)} = \frac{1}{\text{t}}. \tag{B.7}$$

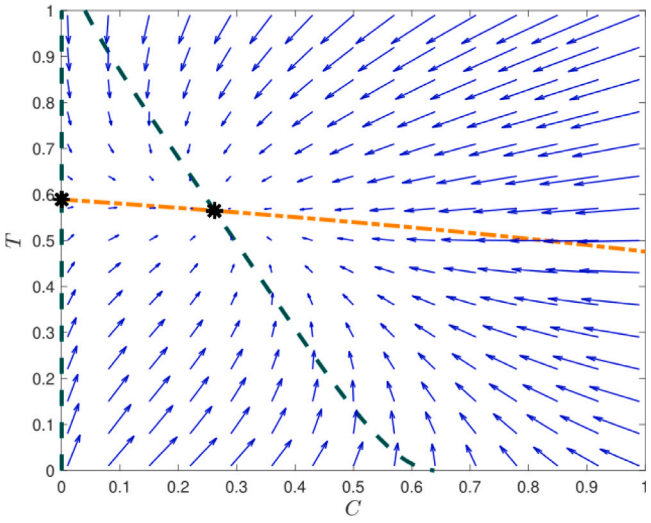

Fig. C.6. Phase portrait of the constant-U model with $U = 1$ (namely, the system of Eqs. (C.1) with the parameter set Σ_A of Table 2). The two asterisks represent the asymptotic equilibria: the left asterisk is X_1 where the only finite population is that of the turf algae, while X_2 is the right asterisk in which the coexistence of turf and *Cystoseira s.l.* takes place. The orange dot-dashed line and the green dashed line are, respectively, the C-isocline and the T-isocline, namely the points of the (C, T) plane at which $\frac{dC}{dt} = 0$ and $\frac{dT}{dt} = 0$ respectively.

When grazing terms are dealt with, in general one should mean

$$f_{CU}(C_\partial) = \frac{A_{CU}^\partial C_\partial}{B_{CU}^\partial + C_\partial},$$

with $[A_{CU}^\partial] = \text{t}^{-1}$ and $[B_{CU}^\partial] = \text{m}$. Considering (B.1) again, after some algebra one has

$$f_{CU}(C_\partial) = \frac{A_{CU}^\partial \sqrt{C}}{\frac{B_{CU}^\partial}{k_n\sqrt{m_C}} + \sqrt{C}}.$$

Provided one defines

$$A_{CU}^{\surd} = A_{CU}^\partial, \quad B_{CU}^{\surd} = \frac{B_{CU}^\partial}{k_n\sqrt{m_C}},$$

and uses the simpler names A_{CU} instead of $A_{CU}^{\surd}$, and B_{CU} instead of $B_{CU}^{\surd}$, one has:

$$\text{(B.3)} \implies [A_{CU}]_{(8)} = \frac{1}{\text{t}}, \quad [B_{CU}]_{(8)} = \sqrt{\text{m}}. \tag{B.8}$$

The use of the same symbols in the bulk model (9) might be misleading, even if things are made simpler this way: in the case of parameters appearing in the system (9), the dimensional equations (B.5), (B.7) and (B.8) will read

$$\begin{cases} [R_{C,T}]_{(9)} = \frac{1}{\text{t}}, \quad [K_{C,T}]_{(9)} = \text{m}, \quad [\beta]_{(9)} = \frac{1}{\text{m t}}, \\ [A_{CU}]_{(9)} = \frac{1}{\text{t}}, \quad [B_{CU}]_{(9)} = \text{m}. \end{cases} \tag{B.9}$$

Appendix C. The 2D sub-model

All the choices mentioned in Section 2.1, namely the algebraic or exponential form of the shadowing factors, and the satiability of sea urchins, give rise to a rich "zoology" of models. In order to examine better the effect of satiability of sea urchins in particular, here we only

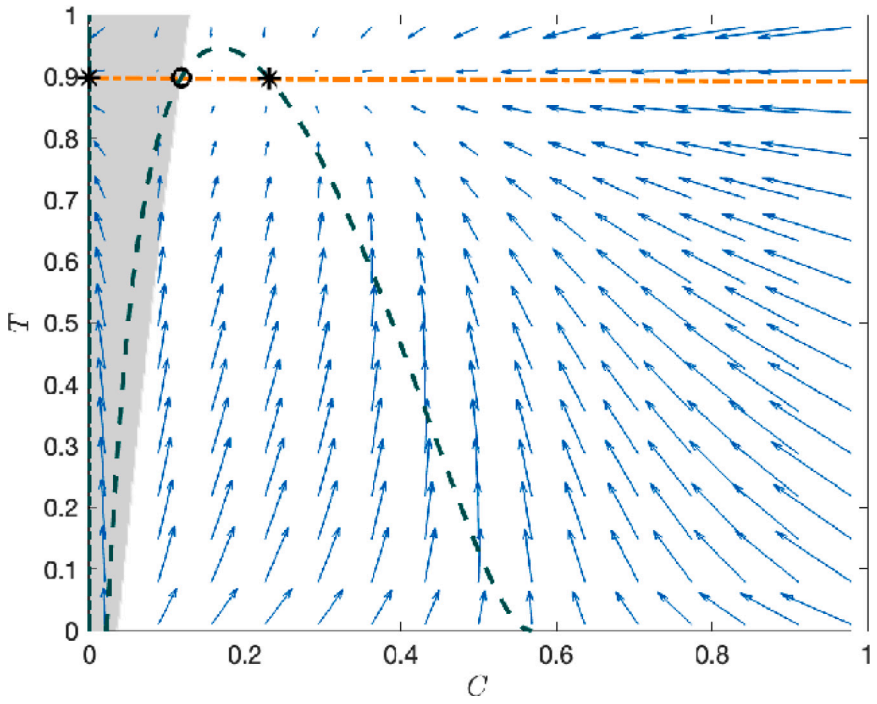

Fig. C.7. Phase portrait of the constant-U version of the model with the choice $U = 0.1$ for the sea urchin constant abundance (namely, the systems of Eqs. (C.2) with the parameter set as in the scenario Σ_B of Table 2). The axis C is the *Cystoseira s.l.* population, the axis T is the turf population. The graphic interpretation is the same as that of Fig. C.6: the two asterisks mark, from left to right, the positions of the two stable equilibria X_1 and X_2, while the circle marks the position of the unstable equilibrium X_3. The choice $U = 0.1$ implies that the stable equilibrium without *Cystoseira s.l.* is reached from a finite region of initial conditions of the (C, T) plane, i.e. the shaded area: this means that there may well exist initial conditions with some Fucales canopy that gets extinct because the sea urchins are too few to contrast the turf competition. The other stable equilibrium, to which the ecosystem converges from outside the shaded region, is the coexistence represented by the right asterisk.

consider *the constant-U model with the algebraic attenuation*, with *either satiable or insatiable sea urchins*.

The constant-U model with insatiable sea urchins is constructed from the system of ODEs (3) by using the response functions in (6) and the attenuation factors in (4), so that the model obtained reads:

$$\begin{cases} \dfrac{dC}{dt} = \left(1 - \dfrac{T}{T_0^*}\right) R_C \sqrt{C} \left(1 - \sqrt{\dfrac{C}{K_C}}\right) - a_{CU}\sqrt{CU} - \beta\sqrt{CT}, \\ \dfrac{dT}{dt} = \left(1 - \dfrac{C}{C_0^*}\right) \Phi \left(1 - \dfrac{T}{K_T}\right) + R_T \sqrt{T} \left(1 - \sqrt{\dfrac{T}{K_T}}\right) - a_{TU} TU. \end{cases} \tag{C.1}$$

The constant-U model with satiable sea urchins is the same, but uses the response functions in (5), and is written as:

$$\begin{cases} \dfrac{dC}{dt} = \left(1 - \dfrac{T}{T_0^*}\right) R_C \sqrt{C} \left(1 - \sqrt{\dfrac{C}{K_C}}\right) - \dfrac{A_{CU}\sqrt{CU}}{B_{CU} + \sqrt{C}} - \beta\sqrt{CT}, \\ \dfrac{dT}{dt} = \left(1 - \dfrac{C}{C_0^*}\right) \Phi \left(1 - \dfrac{T}{K_T}\right) + R_T \sqrt{T} \left(1 - \sqrt{\dfrac{T}{K_T}}\right) - \dfrac{A_{TU} TU}{B_{TU} + T}. \end{cases} \tag{C.2}$$

Let us present then the numerical analysis of this constant-U model. By appropriately selecting the parameters in Eqs. (C.1), the system can be characterized as scenario Σ_A in Table 2. In this scenario, two equilibrium points are found: the first equilibrium $X_1 = (0, T_1)$ describes a system state where the *Cystoseira s.l.* population has gone extinct; the other equilibrium $X_2 = (C_2, T_2)$ represents a coexistence state. The plot in Fig. C.6 represents the vector field $\left(\frac{dC}{dt}, \frac{dT}{dt}\right)$, and also the loci with $\frac{dC}{dt} = 0$ and $\frac{dT}{dt} = 0$ (isocline curves). Two basins of attraction appear. Since the system converges to X_1 only from initial conditions $(0, T)$, this equilibrium turns out to be ecologically unstable. The equilibrium X_2 is instead stable (even if only *quasi-globally*).

From an ecological perspective, the scenario depicted in Fig. C.6 is favorable to the conservation of *Cystoseira s.l.*, as convergence to the C-free equilibrium state X_1 occurs only when the initial condition assumes a zero C population. This advantageous outcome is attributed to the insatiable grazing behavior of sea urchins, which effectively suppress the proliferation of turf-forming algae.

Performing the numerical analysis of the constant-U model with satiable sea urchins in the system (C.2), with parameters choice as in column Σ_B of Table 2, one finds again two equilibria X_1 (with $T \neq 0$ and $C = 0$) and X_2 (co-existence). However, the basin of attraction of X_1 is not simply the axis containing it, but a whole 2D region of the phase space (the gray region in the plot on the right hand side of Fig. C.7). In addition, a third, unstable equilibrium point, denoted X_3, emerges. Under this second scenario, the model reveals a basin of initial conditions in which a sufficiently low initial population of *Cystoseira s.l.* is unable to resist the combined pressures of turf competition and sea urchin grazing. Notably, satiable sea urchins are less effective than their insatiable counterparts in promoting the persistence of *Cystoseira s.l.*, as their grazing is limited to partial foraging along the canopy border, in contrast to their more thorough consumption of turf.

The overall result of constant-U simulations is that a reasonably high population of sea urchins permits the two algal populations to coexist: there is an apparent balance between the one fact that the turf exogenous recruitment may allow for some $\frac{dT}{dt} > 0$ even when T has

gone extinct temporarily, which does not happen for C, and the other fact that sea urchins may graze turf more severely than Fucales.

Data availability

Data will be made available on request.

References

Agnetta, D., Bonaviri, C., Badalamenti, F., Scianna, C., Vizzini, S., Gianguzza, P., 2013. Functional traits of two co-occurring sea urchins across a barren/forest patch system. J. Sea Res. 76, 170–177.

Airoldi, L., 1998. Role of disturbance, sediment stress, and substratum retention on spatial dominance in algal turf. ecology. http://dx.doi.org/10.1890/0012-9658(1998)079[2759:RODSSA]2.0.CO;2.

Ajraldi, V., Pittavino, M., Venturino, E., 2011. Modeling herd behavior in population systems. Nonlinear Anal. Real World Appl. 12, 2319–2338.

Alestra, T., Schiel, D.R., 2015. Impacts of local and global stressors in intertidal habitats: Influence of altered nutrient, sediment and temperature levels on the early life history of three habitat-forming macroalgae. J. Exp. Mar. Biol. Ecol. 468, 29–36. http://dx.doi.org/10.1016/j.jembe.2015.03.017.

Andersen, T., Carstensen, J., Hernández-García, E., Duarte, C.M., 2009. Ecological thresholds and regime shifts: approaches to identification. Trends Ecol. Evol. 24, 49–57.

Ballesteros, E., Sala, E., Garrabou, J., Zabala, M., 1998. Community structure and frond size distribution of a deep water stand of Cystoseira spinosa (Phaeophyta) in the Northwestern Mediterranean. Eur. J. Phycol. 33 (2), 121–128.

Ballesteros, E., Torras, X., Pinedo, S., García, M., Mangialajo, L., de Torres, M., 2007. A new methodology based on littoral community cartography dominated by macroalgae for the implementation of the European water framework directive. Mar. Pollut. Bull. 55, 172–180.

Balvanera, P., Pfisterer, A.B., Buchmann, N., He, J.-S., Nakashizuka, T., Raffaelli, D., Schmid, B., 2006. Quantifying the evidence for biodiversity effects on ecosystem functioning and services. Ecol. Lett. 9, 1146–1156.

Baskett, M.L., Salomon, A.K., 2010. Recruitment facilitation can drive alternative states on temperate reefs. Ecology 91 (6), 1763–1773.

Benedetti-Cecchi, L., Pannacciulli, F., Bulleri, F., Moschella, P.S., Airoldi, L., Relini, G., Cinelli, F., 2001. Predicting the consequences of anthropogenic disturbance: large-scale effects of loss of canopy algae on rocky shores. Mar. Ecol. Prog. Ser. 214, 137–150. http://dx.doi.org/10.3354/meps214137.

Bernal-Ibáñez, A., Cacabelos, E., Triay-Portella, R., Ramalhosa, P., Gestoso, I., 2024. Assessing climatic conditions and biotic interactions shaping the success of Cystoseira foeniculacea early-life stages. J. Phycol. 60, 1485–1497. http://dx.doi.org/10.1111/jpy.13516.

Bestelmeyer, B.T., Ellison, A.M., Fraser, W.R., Gorman, K.B., Holbrook, S.J., Laney, C.M., Ohman, M.D., Peters, D.P.C., Pillsbury, F.C., Rassweiler, A., Schmitt, R.J., S., Sharma., 2011. Analysis of abrupt transitions in ecological systems. Ecosphere 2 (12), 129. http://dx.doi.org/10.1890/ES11-00216.1.

Bevilacqua, S., Airoldi, L., Ballesteros, E., Benedetti-Cecchi, L., Boero, F., Bulleri, F., Cebrian, E., Cerrano, C., Claudet, J., Colloca, F., Coppari, M., Di Franco, A., Fraschetti, S., Garrabou, J., Guarnieri, G., Guerranti, C., Guidetti, P., Halpern, B.S., Katsanevakis, S., Mangano, M.C., Micheli, F., Milazzo, M., Pusceddu, A., Renzi, M., Rilov, G., Sarà, G., Terlizzi, A., 2021. Chapter one - Mediterranean rocky reefs in the Anthropocene: Present status and future concerns. Adv. Mar. Biol. 89, 1–51.

Boada, J., Arthur, R., Alonso, D., Pagès, J.F., Pessarrodona, A., Oliva, S., Ceccherelli, G., Piazzi, L., Romero, J., Alcoverro, T., 2017. Immanent conditions determine imminent collapses: nutrient regimes define the resilience of macroalgal communities. Proc. R. Soc. B 284, 20162814. http://dx.doi.org/10.1098/rspb.2016.2814.

Boccaletti, S., De Lellis, P., et al., 2023. The structure and dynamics of networks with higher order interactions. Phys. Rep. 1018 (1–2), 1–64.

Bonaviri, C., Vega Fernandez, C., Fanelli, G., Badalamenti, F., Gianguzza, P., 2011. Leading role of the sea urchin Arbacia lixula in maintaining the barren state in the southwestern Mediterranean. Mar. Biol. 158 (11), 2505–2513.

Bulleri, F., 2013. Grazing by sea urchins at the margins of barren patches on Mediterranean rocky reefs. Mar. Biol. 160, 2493–2501.

Bulleri, F., Benedetti-Cecchi, L., 2006. Mechanisms of recovery and resilience of different components of mosaics of habitats on shallow rocky reefs. Oecologia 149, 482–492.

Bulleri, F., Pardi, G., Tamburello, L., Ravaglioli, C., 2020. Nutrient enrichment stimulates herbivory and alters epibiont assemblages at the edge but not inside subtidal macroalgal forests. Mar. Biol. 167, 181. http://dx.doi.org/10.1007/s00227-020-03789-5.

Cebrian, E., Tamburello, L., Verdura, J., Guarnieri, G., Medrano, A., Linares, C., Hereu, B., Garrabou, J., Cerrano, C., Galobart, C., Fraschetti, S., 2021. A roadmap for the restoration of Mediterranean Macroalgal forests. Front. Mar. Sci. 8, 709219. http://dx.doi.org/10.3389/fmars.2021.709219.

Cheminée, A., Sala, E., Pastor, J., Bodilis, P., Thiriet, P., Mangialajo, L., Cottalorda, J.-M., Francour, P., 2013. Nursery value of Cystoseira forests for Mediterranean rocky reef fishes. J. Exp. Mar. Biol. Ecol. 442, 70–79.

Collini, D., 2019. A Mathematical Model for Inter-Algal Competition (Master Thesis). Mathematics at the University of Florence (Italy), Available at: https://www.academia.edu/112562651/A_mathematical_model_for_inter_algal_competition.

Colucci, R., Diz-Pita, É., Otero-Espinar, M.V., 2021. Dynamics of a two prey and one predator system with indirect effect. Mathematics 9, 436. http://dx.doi.org/10.3390/math9040436.

Connell, S.D., Foster, M.S., Airoldi, L., 2014. What are algal turfs? Towards a better description of turfs. Mar. Ecol. Prog. Ser. 495, 299–307.

Dunn, R.P., Samhouri, J.F., Baskett, M.L., 2021. Transient dynamics during kelp forest recovery from fishing across multiple trophic levels. Ecol. Appl. 31 (6), e02367.

Érdi, P., Tóth, J., 1989. Mathematical Models of Chemical Reactions: Theory and Applications of Deterministic and Stochastic Models. Manchester University Press.

Fagan, W.F., Cantrell, R.S., Cosner, C., 1999. How habitat edges change species interactions. Amer. Nat. 153 (2), 165–182.

Falace, A., Kaleb, S., De La Fuente, G., Asnaghi, V., M., Chiantore, 2018. Ex situ cultivation protocol for Cystoseira amentacea var. stricta (Fucales, Phaeophyceae) from a restoration perspective. PLoS One 13 (2), e0193011.

Fanelli, D., Piazza, F., 2020. Analysis and forecast of COVID-19 spreading in China, Italy and France. Chaos Solitons Fractals: X 134, 109761.

Fasano, A., Primicerio, M., 1979. Free boundary problems for nonlinear parabolic equations with nonlinear free boundary conditions. J. Math. Anal. Appl. 72, 247–273.

Gorman, D., Connell, S.D., 2009. Recovering subtidal forests in human-dominated landscapes. J. Appl. Ecol. 46 (6), 1258–1265.

Gunderson, L.H., 2000. Ecological resilience - in theory and application. Annu. Rev. Ecol. Syst. 31 (1), 425–439.

Holling, C.S., 1973. Resilience and stability of ecological systems. Annu. Rev. Ecol. Syst. 4, 1–23.

House, T., 2012. Modelling epidemics on networks. Contemp. Phys. 53 (3), 213–225.

Humphries, A.T., McClanahan, T.R., McQuaid, C.D., 2020. Algal turf consumption by sea urchins and fishes is mediated by fisheries management on coral reefs in Kenya. Coral Reefs 39, 1137–1146. http://dx.doi.org/10.1007/s00338-020-01943-5.

Karatayev, V.A., Baskett, M.L., 2020. At what spatial scales are alternative stable states relevant in highly interconnected ecosystems? Ecology 101 (2), e02930.

Knowlton, N., 2004. Multiple stable states and the conservation of marine ecosystem. Prog. Oceanogr. 80 (60), 387–396.

Konar, B., Estes, J.A., 2003. The stability of boundary regions between kelp beds and deforested areas. Ecology 84 (1), 174–185.

Krumhansl, K.A., et al., 2016. Global patterns of kelp forest change over the past half-century. PNAS 113 (48), 13785–13790. http://dx.doi.org/10.1073/pnas.1606102113.

Lardi, P.I., Varkitzi, I., Tsiamis, K., Orfanidis, S., Koutsoubas, D., Falace, A., Salomidi, M., 2022. Early development of Gongolaria montagnei (Fucales, Phaeophyta) germlings under laboratory conditions, with a view to enhancing restoration potential in the eastern Mediterranean. Bot. Mar. 65 (4), 279–287.

Lauzon-Guay, J.S., Scheibling, R.E., Barbeau, M.A., 2009. Modelling phase shifts in a rocky subtidal ecosystem. Mar. Ecol. Prog. Ser. 375, 25–39.

Ling, S.D., Kriegisch, N., Woolley, B., Reeves, S.E., 2019. Density-dependent feedbacks, hysteresis, and demography of overgrazing sea urchins. Ecology 100 (2), e02577.

Ling, S.D., Scheibling, R.E., Rassweiler, A., Johnson, C.R., Shears, N., Connell, S.D., Salomon, A.K., Norderhaug, K.M., Pérez-Matus, A., Hernández, J.C., Clemente, L.K., Hereu, B., Ballesteros, E., Sala, E., Garrabou, J., Cebrian, E., Zabala, M., Fujita, D., Johnson, L.E., 2015. Global regime shift dynamics of catastrophic sea urchin overgrazing. Phil. Trans. R. Soc. B. http://dx.doi.org/10.1098/rstb.2013.0269.

Mangialajo, L., Chiantore, M., Susini, L., Meinesz, A., Cattaneo-Vietti, R., Thibaut, T., 2012. Zonation patterns and interspecific relationships of fucoids in microtidal environments. J. Exp. Mar. Biol. Ecol. 412, 72–80.

Marzloff, M.P., Johnson, C.R., Little, L.R., Soulié, J.C., Ling, S.D., Frusher, S.D., 2013. Sensitivity analysis and pattern-oriented validation of TRITON, a model with alternative community states: insights on temperate rocky reefs dynamics. Ecol. Model. 258, 16–32.

Materassi, M., 2019. Some fractal thoughts about the COVID-19 infection outbreak. Chaos Solitons Fractals X 4, 100032.

May, R.M., 1974. Model Ecosystems. Princeton University Press, Princeton, New Jersey.

Melis, R., Ceccherelli, G., Piazzi, L., Rustici, M., 2019. Macroalgal forests and sea urchin barrens: structural complexity loss, fisheries exploitation and catastrophic regime shifts. Ecol. Complex. 37, 32–37. http://dx.doi.org/10.1016/j.ecocom.2018.12.005.

Molinari-Novoa, E., Guiry, M., 2020. Reinstatement of the genera Gongolaria Boehmer and Ericaria Stackhouse (Sargassaceae. Phaeophyceae). Not. Algarum 172, 1–10.

Ortiz, M., Uribe, R.A., 2021. Comparing the stability of successional transient models in kelp forests and barrens (south-east Pacific): Implications for conservation monitoring. Aquat. Conserv.: Mar. Freshw. Ecosyst. 31, 1297–1310.

Pages, J.F., Gera, A., Romero, J., Alcoverro, T., 2014. Matrix composition and patch edges influence plant-herbivory interactions in marine landscapes. Funct. Ecol. 28, 1440–1448.

Palacìn, C., Giribet, G., Carner, S., Dantart, L., Turon, X., 1998. Low densities of sea urchins influence the structure of algal assemblages in the western Mediterranean. J. Sea Res. 39, 281–290.

Petraitis, P.S., Latham, R.E., 1999. The importance of scale in testing the origins of alternative community states. Ecology 80 (2), 429–442.
Piazzi, L., Balata, D., Ceccherelli, G., 2017. Resilience of cystoseira beds: lack of canopy effects on recruitment. Bot. Mar. 60, 49–53.
Piazzi, L., Ceccherelli, G., 2019. Effects of sea urchin human harvest in promoting canopy-forming algae restoration. Estuar. Coast. Shelf Sci. 219, 273–277.
Pinna, S., N., Sechi., Ceccherelli, G., 2013. Canopy structure at the edge of seagrass affects sea urchin distribution. Mar. Ecol. Prog. Ser. 485, 47–55.
Ratajczak, Z., Carpenter, S.R., Ives1, A.R., Kucharik, C.J., Ramiadantsoa, T., Stegner, M.A., Williams, J.W., Zhang, J., Turner, M.G., 2018. Abrupt change in ecological systems: Inference and diagnosis. Trends Ecol. Evol. 33 (7), 513–526.
Ries, L., Fletcher, R.J., Battin, J., Sisk, T.D., 2004. Ecological responses to habitat edges: mechanisms, models, and variability explained. Annu. Rev. Ecol. Evol. Syst. 35, 491–522.
Rocha, J.C., Peterson, G.D., Biggs, R., 2015. Regime shifts in the anthropocene: drivers, risks, and resilience. PLoS One 10 (8), e0134639.
Rustici, M., Ceccherelli, G., Piazzi, L., 2017. Predator exploitation and sea urchin bistability: consequence on benthic alternative states. Ecol. Model. 344, 1–5.
Sala, E., Ballesteros, E., Dendrinos, P., Di Franco, A., Ferretti, F., Foley, D., Fraschetti, S., Friedlander, A., Garrabou, J., Gülüsoy, H., Guidetti, P., Halpern, B.S., Hereu, B., Karamanlidis, A.A., Kizilkaya, Z., Macpherson, E., Mangialajo, L., Mariani, S., Micheli, F., Pais, A., Riser, K., Rosenberg, A.A., Sales, M., Selkoe, K.A., Starr, R., Tomas, F., Zabala, M., 2012. The structure of Mediterranean rocky reef ecosystems across environmental and human gradients, and conservation. PLoS One 7 (2), e32742.
Scheffer, M., Carpenter, S., Foley, J.A., Folke, C., Walker, B., 2001. Catastrophic shifts in ecosystems. Nature 413 (6856), 591–596.
Selkoe, K.A., Blenckner, T., Caldwell, M.R., Crowder, L.B., Erickson, A.L., Essington, T.E., Estes, J.A., Fujita, R.M., Halpern, B.S., Hunsicker, M.E., et al., 2015. Principles for managing marine ecosystems prone to tipping points. Ecosyst. Heal. Sustain. 1 (5), 1–18. http://dx.doi.org/10.1890/EHS14-0024.1.
Strain, A.M.A., Thomson, R.J., Micheli, F., Mancuso, F.P., Airoldi, L., 2014. Identifying the interacting roles of stressors in driving theglobal loss of canopy-forming to mat-forming algae inmarine ecosystems. Global Change Biol. 20, 3300–3312. http://dx.doi.org/10.1111/gcb.12619.
Tamburello, L., Papa, L., Guarnieri, G., Basconi, L., Zampardi, S., Scipione, M.B., et al., 2019b. Are we ready for scaling up restoration actions? An insight from Mediterranean macroalgal canopies. PLoS One 14 (10), e0224477. http://dx.doi.org/10.1371/journal.pone.0224477.
Tamburello, L., Ravaglioli, C., Mori, G., Nuccio, C., Bulleri, F., 2019a. Enhanced nutrient loading and herbivory do not depress the resilience of subtidal canopy forests in Mediterranean oligotrophic waters. Mar. Environ. Res. 149, 7–17.
Thibaut, T., Blanfune, A., Boudouresque, C., Verlaque, M., 2014. Decline and local extinction of fucales in French Riviera: the harbinger of future extinctions? Med. Mar. Sci. 16 (1), 206–224.
Thibaut, T., Pinedo, S., Torras, X., Ballesteros, E., 2005. Long-term decline of the populations of fucales (Cystoseira spp. and sargassum spp.) in the Albères coast (France, north-western Mediterranean). Mar. Pollut. Bull. 50, 1472–1489.
Thiriet, P.D., Di Franco, A., Cheminee, A., Guidetti, P., Bianchimani, O., Basthard-Bogain, S., et al., 2016. Abundance and diversity of crypto- and necto-benthic coastal fish are higher in marine forests than in structurally less complex macroalgal assemblages. PLoS One 11, e0164121.
Verdura, J., Sales, M., Ballesteros, E., Cefalì, M.E., E., Cebrian, 2018. Restoration of a canopy-forming alga based on recruitment enhancement: Methods and long-term success assessment. Front. Plant Sci. 9 (4), 1832.
Wernberg, C., 2008. Physical disturbance and subtidal habitat structure on open rocky coasts: effects of wave exposure, extent and intensity. J. Sea Res. 59, 237–248.
Wilman, E.A., 2021. Kelp forests: Catastrophes, resilience, and management. Front. Ecol. Evol. 9, 674792. http://dx.doi.org/10.3389/fevo.2021.674792.
Worm, B., et al., 2006. Impacts of biodiversity loss on ocean ecosystem services. Science 314, 787–790. http://dx.doi.org/10.1126/science.1132294.